

JULY 1982

HEWLETT-PACKARD JOURNAL



Contents:

- 3 Optical System Design for the Laser Printing System**, by John R. Lewis and Laurence M. Hubby, Jr. *The goal was to optimize printing speed and resolution consistent with economy of production, data rate, and process parameters.*
- 5 Laser Printer Optics Control and Diagnostic Circuit**, by Gary L. Holland *This system drives the laser-beam modulator and checks the optics module.*
- 8 A Synchronous Mirror-Motor Drive for the Laser Printer**, by Gary L. Holland *The scanning mirror sweeps the laser beam across the page. This circuit keeps it turning at constant speed.*
- 11 Laser Printer Machine Control System**, by James D. Crumly and Von L. Hansen *This microprocessor system controls everything in the laser printer except data formatting.*
- 13 Sensing Paper Jams**, by Gary L. Holland *If the paper drive motor is going too fast or too slowly, the paper may have jammed or torn.*
- 16 Solid-State Microwave Signal Generators for Today's Exacting Requirements**, by Donald R. Chambers and Steven N. Sanders *They have excellent spectral purity, high accuracy, versatile modulation capabilities, and powerful self-test features.*
- 20 High-Performance Wideband Cavity-Tuned Solid-State Oscillators**, by Edward G. Cristal, Arthur N. Woo, Phillip G. Foster, and Ronald F. Stiglich *These novel designs use a pair of oscillator circuits coupled into a single high-accuracy tunable cavity.*
- 26 A Wide-Dynamic Range Pulse Leveling Scheme**, by James F. Catlin *This design provides leveled output power over a range of 145 dB for both CW signals and pulses as narrow as 100 nanoseconds.*
- 30 Microwave Solid-State Amplifiers and Modulators for Broadband Signal Generators**, by Kim Potter Kihlstrom *Basic hybrid microcircuit designs are customized for each of four signal generator models.*

In this Issue:



How do you replace an act that's been playing for twenty years and is still drawing plenty of customers? Engineers at HP's Stanford Park Division had to find the answer when they set out to design replacements for HP's long-lived line of klystron signal generators. These generators are much prized by customers who need tunable sources of pure stable microwave frequencies. In each generator is a klystron oscillator tube, its frequency of oscillation determined by a mechanically tuned microwave cavity (a metal-enclosed space of controlled size and shape). The cavity-klystron combination is hard to beat for spectral purity, but it makes for a big, unwieldy package, and just about any twenty-year-old design can be improved by applying the latest technology. The engineers kept the cavity tuning, replaced the klystrons with transistors, added a microprocessor, applied up-to-date circuit design techniques and some novel ideas, implemented many critical circuits as state-of-the-art microcircuits, and gave us the new 8683A/B and 8684A/B Microwave Signal Generators. The project took a long time because it wasn't easy to match that klystron spectral purity, but the new generators do match it and surpass the old generators in every other performance area. You'll find an overview of the new generators on page 16, a description of the cavity-tuned oscillators on page 20, and other design articles on pages 26 and 30. Our cover photograph this month shows the disassembled cavity and tuning mechanism in front of the 8684B Signal Generator. The cavity mechanism lives behind the knob on the left side of the front panel.

Pages 3 through 15 of this issue complete our coverage of the 2680 Laser Printing System. Last month's issue was entirely devoted to this versatile, cost-effective computer output printer. This month you can read about the optical system that guides the laser beam on its path from the laser to the photoconductive drum, and about the machine control system, the microprocessor-based electronic subsystem that monitors and controls the printer.

In this year's January issue we enclosed a reader opinion questionnaire. Our computer has now digested the returns and is beginning to give us data that will help shape the future of the Hewlett-Packard Journal. Worldwide, about 4% of our readers returned the questionnaire. Many enclosed notes and letters. We were pleased to find that 49% of our readers have been with us more than five years and 53% file the Journal for reference. To those who shared their opinions with us, our sincere thanks.

-R. P. Dolan

Optical System Design for the Laser Printing System

Here are the details of the optical system of the 2680 Laser Printing System described in these pages last month.

by John R. Lewis and Laurence M. Hubby, Jr.

THE OPTICAL SYSTEM of the 2680 Laser Printing System is designed to provide the highest resolution and printing speed possible consistent with reasonable economy of production, the data rate capability of the digital electronics, and the properties of the electrophotographic process. A variety of factors influenced the choice of each component and the configuration chosen for each portion of the design.

In the optical system, light from a laser source is shaped into a spot of the desired diameter at the photoconductor drum by the scan lens. Action of the scanner produces a line scan across the drum, forming the horizontal portion of a high-resolution raster scan. The rotation of the drum provides the vertical scan. A stream of information is impressed upon the light beam by the modulator in response to commands from the character processor.

The scanning system is required to produce a spot of accurate size that yields the required developed dot diameter. The length of the scan line produced must be sufficient to cover the desired copy size (European A4 paper, 210×297 mm), and thus a number of resolvable spots equal to the ratio of these two quantities is required. Laser power should be sufficient to allow copy to be produced as fast as permitted by either the electrophotographic process or the rate at which data can be written, whichever is more restrictive, and the capabilities of the scanner and modulator must be consistent with this speed.

Laser and Process Characteristics

A helium-neon laser was chosen for several reasons. First, the demonstrated maintenance-free life of hard-sealed helium-neon lasers (20,000 hours) is three to ten times longer than that of any of the other candidates, while its initial cost is of the order of ten times lower. Second, the size and power consumption of these units are modest, particularly compared to devices such as ion lasers. Third, the wavefront quality produced by the device is excellent, and fourth, the photoconductor sensitivity at the HeNe emission wavelength (633 nm) is good.

The dot placement resolution used in the 2680A is 141 μm , corresponding to an optical dot size of about 125 μm , and the exposure required is about 1.5 microjoules per square centimetre, corresponding to an optical energy required for each dot of $1.85 \times 10^{-4} \mu\text{J}$. A five-milliwatt laser is used, allowing dots to be written at a rate given by:

$$\begin{aligned} \text{Rate} &= (5 \times 10^3 \mu\text{J/s}) / (1.85 \times 10^{-4} \mu\text{J/dot}) \\ &= 2.71 \times 10^7 \text{ dots/s} \end{aligned}$$

The actual writing rate cannot be this high because the optical system has an overall transmission of about 35%, and a safety margin of roughly another factor of 1.5 must be allowed to account for the decrease in the laser's power over its useful life. The required dot rate is thus something less than 6×10^6 dots/second, corresponding to a data rate of about 0.75 megabytes/second. The five-milliwatt laser is quite adequate for these numbers. This is fortunate because the price and physical size of helium-neon lasers increase dramatically as the output power exceeds five milliwatts.

The helium-neon laser requires an external modulator for such data rates, and devices operating on two different principles were given consideration: acousto-optic and electro-optic. The data rates required are a problem for neither. However, the acousto-optic modulator is free from thermal drift effects which cause the electro-optic device to require periodic readjustment, is more compact and cheaper, will work with unpolarized light without causing additional loss, and does not require high-voltage components in its driver. It was therefore the obvious choice.

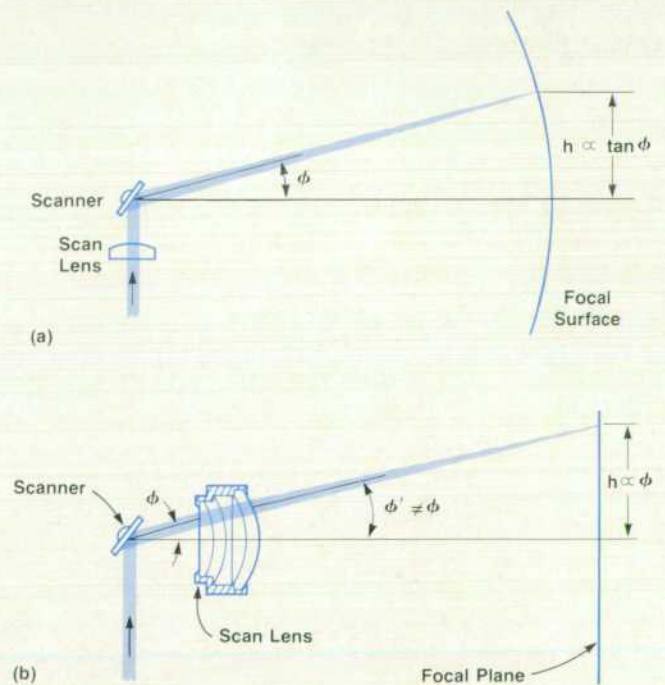


Fig. 1. (a) Postobjective scanning. (b) Preobjective scanning. The 2680A Laser Printer uses (a).

Scanning Method

The scanning system consists of two major parts, the scan objective lens and the scanner. The order in which the beam encounters these two components as it progresses toward the final image plane forms the basis for the usual classification of scanning systems as either postobjective or preobjective. Postobjective scanning is shown in Fig. 1a, and is attractive because only a very simple scan lens is required (frequently just a single element). The arrangement has the disadvantage, however, of producing a curved focal surface. Preobjective scanning, shown in Fig. 1b, requires a much more complex scan lens, but this complexity can then be exploited to produce not only a flat focal plane, but one corrected for angular distortions as well. The major factors that determine which configuration must be used are the system resolution and overall size constraints. As shown in Fig. 2a, a laser beam near focus remains nearly constant in diameter for a finite distance, called the depth of field, and this distance increases as the square of the f-number of the lens that produces the focus. Since the size of the focused spot also depends upon this same quantity, the lens f-number and hence the depth of field are determined by resolution requirements and the wavelength of the laser light. If the resulting depth of field is large enough and/or the scanning system can be located sufficiently far from the scan plane, a curved focal surface can be tolerated, as shown in Fig. 2b, and postobjective scanning may be used. In the case of the 2680A, the required spot size is $125 \mu\text{m}$ and the laser wavelength is $0.6328 \mu\text{m}$. Thus:

$$\begin{aligned} \text{scan lens f-number} &= (125 \mu\text{m}) / (1.64 \times 0.6328 \mu\text{m}) \\ &= 120 \end{aligned}$$

Therefore:

$$\begin{aligned} \text{depth of field} &\approx (4 \times 0.6328 \mu\text{m}) \times 120^2 \\ &\approx 36.4 \text{ mm} \end{aligned}$$

Using the geometry of Fig. 2b and allowing a factor of roughly two for tolerance buildup in the remainder of the system, we could then place the scanning system about 850 mm from the photoconductor drum, corresponding to a scan half-angle of about 10 degrees. The difference between x and $\tan(x)$ at this angle is only about 1%, and thus the angular distortion shown in Fig. 1a would be so small as to need no correction or only very slight correction. These are reasonable numbers, and such a basic layout was chosen for the 2680A scanning system.

The specifications the scanner must meet have by now been fairly well defined, either directly or indirectly. The scanner must resolve a number of spots given by:

$$\begin{aligned} \text{number of spots} &= \text{length of scan line} \div \text{spot size} \\ &= (289 \text{ mm}) / (141 \times 10^{-3} \text{ mm}) \\ &= 2048 \text{ spots} \end{aligned}$$

within the aforementioned scan angle of about 20 degrees. The lines must be scanned at a rate that corresponds to a maximum dot rate of about 6×10^6 dots/s. Also, the scanning system has a finite duty cycle (fraction of time spent printing). Assuming a duty cycle of 46%, the line scan rate is approximately:

$$\begin{aligned} \text{line scan rate} &= (0.46)(6 \times 10^6 \text{ dots/s}) / (2048 \text{ dots/line}) \\ &= 1350 \text{ lines/s} \end{aligned}$$

The performance of scanners based upon rotating polygonal mirrors, single mirrors attached to galvanometers, acousto-optic interactions, and the electrooptic effect in certain crystals were considered in light of the above requirements, and it quickly became obvious that only the first of these devices could achieve both the required resolution and scan rate comfortably at a reasonable cost. The electrooptic devices are not capable of enough spots. Acousto-optic deflectors have been reported with up to 10,000-spot capability, but these devices are complex and expensive. Mirrored galvanometers are capable of enough spots, but can only achieve the required scan rate in resonant systems. This would require the scan velocity to vary sinusoidally, resulting in line-linearity and exposure-level variations that would be unacceptable unless the field were very substantially overscanned. Since such overscanning would require an unacceptably low duty cycle, galvanometers were eliminated from consideration.

Wobble Correction

Rotating polygon scanners are not without their problems, however. Primary among them is pyramid error in the orientation of the individual facets of the polygon. This type of defect causes the light reflected from successive facets to arrive at the scan plane at different locations in the direction perpendicular to that of the scan. Since successive facets correspond to successive scan lines on the drum,

(continued on page 6)

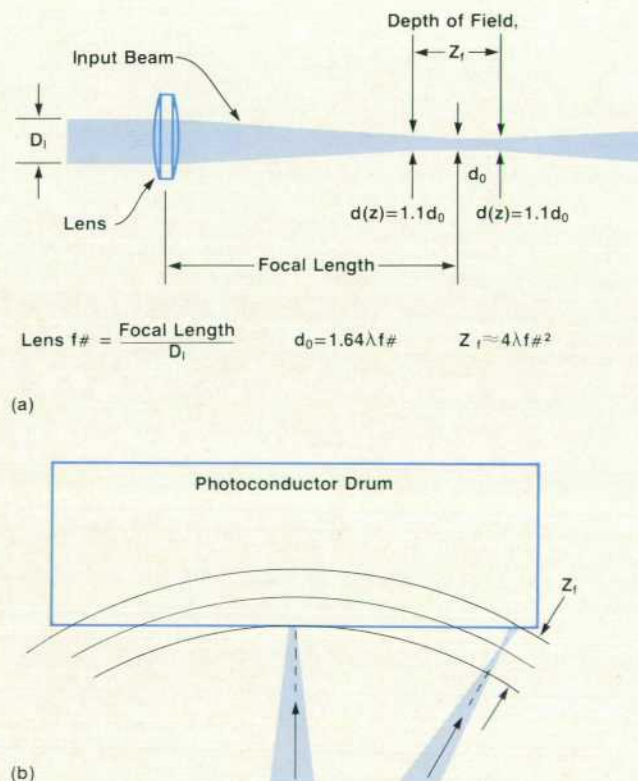


Fig. 2. If the depth of field of the focused laser beam is sufficient, a curved focal surface can be tolerated.

Laser Printer Optics Control and Diagnostic Circuit

by Gary L. Holland

Within the 2680A Laser Printer's optics casting is the optics control and diagnostic circuit, which performs the following functions:

- It drives the acoustooptic modulator with variable RF power to allow analog modulation of the laser beam as well as on/off control.
- It monitors the RF power driving the acoustooptic modulator.
- It monitors the laser power deflected onto the drum.
- It provides a synchronization signal to align data correctly for successive scans across the drum.

Acoustooptic Modulator Driver

This section of the circuit modulates an 80-MHz signal to the acoustooptic modulator (Fig. 1). The machine control system (MCS) processor sets the laser power through a digital-to-analog converter (DAC). Intensity setting 00 corresponds to low RF power into the laser modulator and hence low laser power. Increasing intensity values result in increasing RF power into the modulator. This results in increased optical power up to the point when the laser modulator saturates, and then optical power begins to fall off. This saturation point varies from modulator to modulator. The on/off signal VIDEO enables the RF power when high and disables it when low. The 80-MHz oscillator consists of an ECL gate, a crystal, and tank and loading circuits. The signal from this oscillator is modulated with a diode modulator. The amount of 80-MHz signal going through the modulator is roughly proportional to the current drawn from the modulator by the programmable current source, which is set by the machine control processor. When VIDEO is low, a switchable current source provides current to the RF modulator and the programmable current source, and the RF modulator is reverse-biased so that no signal goes through the modulator. When VIDEO is high, the switchable current source is turned off, and the programmable current source then sinks current out of the RF modulator, turning it on and allowing a preset amount of 80-MHz power to go into the acoustooptic modulator.

The output amplifier that drives the acoustooptic modulator is a hybrid amplifier. Its output is monitored by a peak detector. A fraction of the peak value is buffered and sent to the machine control system to indicate to the MCS the magnitude of the RF power.

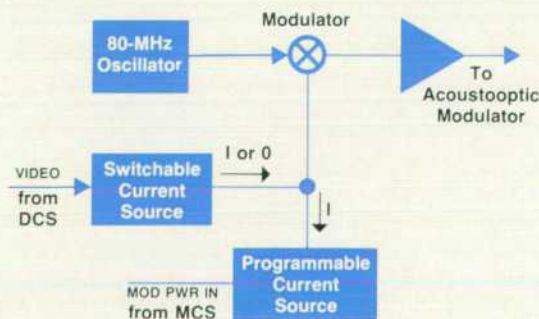


Fig. 1. Acoustooptic modulator driver.

Beam Detection and Laser Monitoring

The beam-detect section (Fig. 2) monitors the first-order power and detects when the beam sweeps across the beam-detect diode. The first-order power is the portion of the laser power deflected through the acoustooptic modulator when RF power is applied to it by the modulator driver section. The first-order power is monitored only as the beam sweeps past the beam-detect diode. An amplifier buffers the signal and a peak detector produces a voltage proportional to the power into the beam-detect diode. The peak voltage is called FIRST-ORDER POWER. This signal is divided by 2 and compared with the buffered output from the beam-detect diode. When this output passes through its half-peak points, a comparator switches and the driver sends this switched signal back to the data control system. This signal is called BEAM DETECT and is the horizontal sync signal.

The machine control processor uses the FIRST-ORDER POWER signal to monitor the amount of laser power going onto the drum. The MCS can then alter this power by altering the amount of RF power sent to the acoustooptic modulator as explained above.

Diagnostics

The optics diagnostics are executed in the print mode once per drum revolution when the drum seam is in front of the modulated beam. The two parameters that are measured with the analog-to-digital converter and used for fault detection are FIRST-ORDER POWER (FOP) and RF driver output power (MOD PWR OUT).

To prevent possible safety hazards, the RF output power going into the acoustooptic modulator is monitored with the RF driver turned off. This is monitored both in and out of the print mode. If any RF power is detected when the laser should be off, the laser power supply is disabled, the ac contactor is opened, and the +28-volt supply is disabled.

The following is a list of all the possible optics failures in the order in which they are detected: 1) RF driver stuck on, 2) RF driver failure, 3) scanner failure, 4) beam detect failure, 5) scanner start failure. Some of the failures require the electrostatic loop potentials to be out of range before a failure is flagged. If the loop is limited, a warning message is displayed. In the service command mode the warnings are flagged whether the loop is limited or not. This applies to RF driver failures and beam-detect failures.

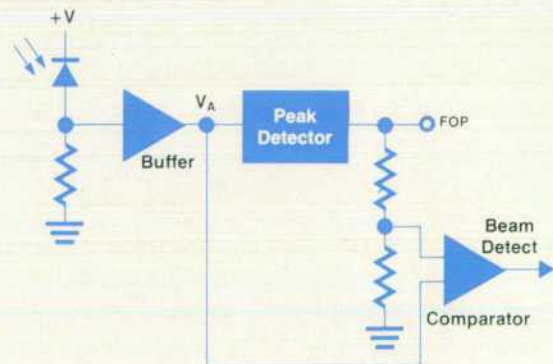


Fig. 2. Beam detection circuit.

printed copy produced with a scanner exhibiting this problem contains periodic errors in the vertical placement of the dots that form the characters, a condition we call wobble. Controlling wobble by decreasing the residual pyramid error in the polygon during manufacture can be an expensive proposition, since the angular accuracy required is of the order of one second of arc. Fortunately, an optical solution to the wobble problem exists, as shown in Fig. 3. If the beam is brought to a focus in the direction perpendicular to that of the scan at the face of the polygon and then refocused to its original form after deflection, the vertical position of the beam at the scan plane will be independent of pyramid error in the polygon, and hence the final print will exhibit no wobble. The lenses involved must, of course, be sufficiently well corrected to maintain the required final spot size as well as the action just described over the range of motion of the scanner. This is not a trivial requirement for the lens that follows the scanner, particularly if preobjective scanning is used and this lens must form the final spot in the scan direction as well. As shown in Fig. 4, the natural form for this lens is toroidal, essentially that of a cylinder lens bent into an arc so as to be equidistant from the polygon face at all points in the scan. Such lenses can be built, either with conventional glassworking or plastic injection molding techniques. However, the accuracy necessary to achieve good performance is difficult and therefore expensive to maintain.

A viable solution from a cost standpoint would be to use a simple cylinder lens following the scanner, and if the scan angle could be held to small enough values, this would be acceptable optically as well. Unfortunately, the scan half-angle would have to be reduced to less than three degrees, which would increase both the scanner-to-scan-plane distance and the polygon size to unreasonable values. The solution developed for use in the 2680A is shown in Fig. 5. Two additional lenses, which use only spherical surfaces and form essentially a unity-magnification Galilean telescope, surround the simple cylinder lens and create a region in which the scan is angularly compressed. An alternative description is that the apparent source of the light that passes through the cylinder lens is now a distant image of the active polygon facet produced by the first additional lens. The second spherical lens then reimages the scanner to the original apparent distance from the scan plane. The result is that the maximum angle at which the beam must pass through the cylinder lens is sufficiently reduced that

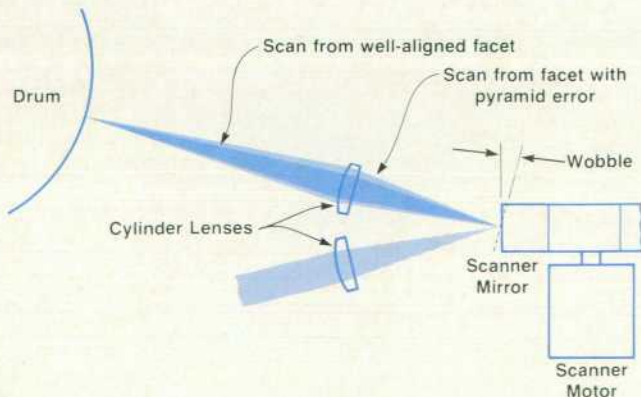


Fig. 3. Wobble correction.

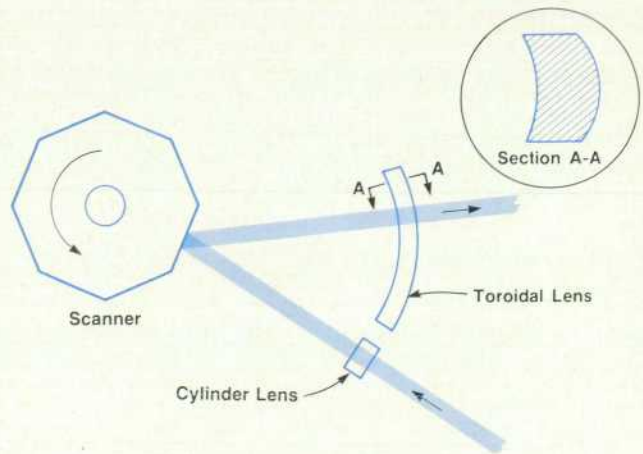


Fig. 4. Toroidal lens form for wobble correction.

satisfactory optical performance is maintained over the entire length of the scan, and yet the system is simpler and less costly than it would be if preobjective scanning were used. The system has the additional benefit of naturally tending to flatten the focal surface, since the beam passes through a greater thickness of glass at the extremes of the scan than it does in the center. The final design of the 2680A scanning system produces an almost completely flat focal surface, making the entire depth of field available to compensate for tolerance buildup elsewhere in the system.

2680A Optical System

The complete 2680A optical system, shown in Fig. 6, contains a few other components whose functions are perhaps best explained by following the beam through the system. Light leaving the laser first encounters a lens which produces a spot of appropriate size in the modulator crystal to obtain the optimum compromise between speed and efficiency in this device. The modulator, in effect, turns the beam on by deflecting it through a negative lens whose purpose is to expand the beam in a reasonable distance to the diameter required by the combination of the scan lens f-number and working distance. The beam next encounters the single-element scan lens, which causes it to converge toward a focus at roughly the drum location. A short distance farther along the path is the first wobble-correcting cylinder lens, which focuses the beam to a line focus in the

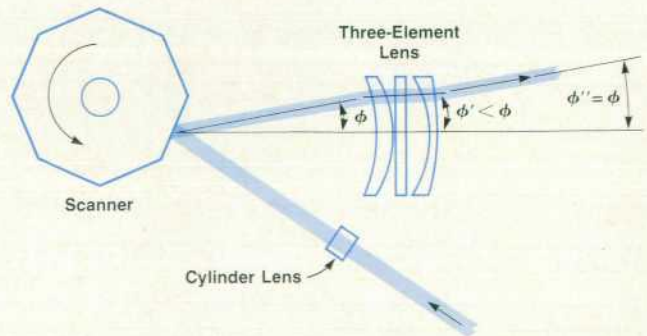


Fig. 5. The 2680A Laser Printer uses a three-element lens for wobble correction.

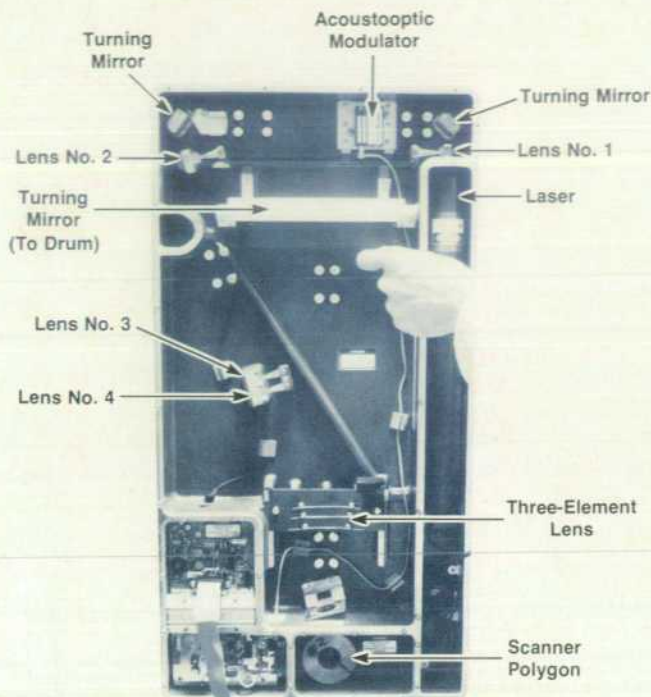


Fig. 6. 2680A Laser Printer optical system.

plane of the page on the active facet of the polygon. The polygon has 18 sides, giving a total scan angle of 40 degrees, about half of which is used for writing. The remainder allows time for the apexes of the polygon to pass through the beam and a beginning-of-scan sync mark to be detected. The polygon measures 60 mm between opposite faces and turns at 4500 r/min. After reflecting from the polygon, the beam passes through the set of three lenses described above—spherical, cylindrical, and spherical—which complete the wobble correction. This group is placed a distance from the polygon that yields a slightly elliptical final spot whose minor axis is aligned with the direction of scan. This helps obtain a round printed dot because it partially compensates for the blurring effect of the motion of the beam during exposure. After the final lens group, the beam is reflected through 90 degrees by a long turning mirror and passed through a window out of the optics assembly toward the photoconductor drum. A mirror intercepts the beam shortly before it reaches the beginning of each scan line and reflects it to a photodetector which generates the scan sync signal.

Mechanical Design Considerations

The optics assembly is designed to be a field-replaceable module with no adjustments required. This means that the alignment between the optics assembly and the rest of the printing process is critical and must be as free as possible from product assembly errors or tolerance buildup. The mounting details for the optics module are on the process module, and the resulting assembly is suspended from the main machine frame in such a way as to be relatively independent of gross frame errors.

The requirements of optical alignment between modules do impose special requirements on the machine structure. If special installation leveling and adjustments are to be avoided, the frame must be stiff enough to hold the required alignment geometry over the full range of weight distribution between casters or levelers. This requirement was met with a welded box tube base and a welded steel channel frame. This design holds the required optical alignments even if one of the front casters is completely off the ground. This means that no special installation alignment is required, although it is recommended that the levelers be nearly evenly loaded for best results.

The process module is a very dirty environment with loose, statically charged, black toner dust and paper dust, and blowing, rubbing, and throwing mechanisms to distribute it all over. To protect the optics from this environment, and to protect the operator and service person from the laser beam, a conduit contains the output beam between the optics module and the point in the printing process where the light is used. A window on the optics module keeps air flows and contaminants from the interior of the module, and a small blower draws in filtered air to keep the conduit at a positive pressure with respect to the sources of contamination. This system also reduces contamination on other critical process components.

Layout and Folding

The long-focal-length lenses used in the optics result in a path length of 2.3 metres from the end of the laser to the spot on the drum. The scanning mirror and two other mirrors fold this optical path into a reasonable-size package 366 by 712 by 72 mm. Vertical placement of the package along one side of the machine uses the interior space of the machine efficiently.

Since the system uses long focal-length lenses, it is relatively tolerant of errors in element placement along the optic axis. As a result, it was possible to eliminate all lens adjustments in the direction of the optic axis. This approach requires more care in lens fabrication and location, but results in fewer parts, more reliability, faster assembly, and simpler alignment. Each lens is located by fixed details in a machined housing. Only the folding mirrors and the modulator Bragg angle* are adjustable.

The long focal length of the lenses and the resulting long path are disadvantages in that they increase the sensitivity of the assembly to torsional deflections. A sand casting was chosen to form the base of the module because of its relative stability and stiffness. Even with a rigid casting as the reference for the assembly, it is important to avoid any torsional loading on the module. As a result, the attachment to the rest of the machine uses just three mounts so that distortions of the rest of the machine tend only to mislocate the housing and not to twist it.

Lens and Laser Mounts

The first four lenses and the laser are held against the sides and bottoms of machined slots in the casting with simple leaf springs (Fig. 7). These lenses are thick and have well specified mechanical-to-optical tolerances so they can

*Bragg angle is a characteristic angle at which light rays reflect from planes of atoms in a crystal.

A Synchronous Mirror-Motor Drive for the Laser Printer

by Gary L. Holland

In the optics assembly of the HP 2680A Laser Printer, a motor spins the polygon mirror to sweep the laser beam across the page. The scanner motor is driven at a constant angular velocity of 75 revolutions per second.

The armature of the motor is the stator and the field is supplied by a permanent magnet in the rotor. By sequentially energizing the coils in order of phase number, a rotating magnetic field is created in the stator. Under normal operating conditions, the magnet (the rotor) follows this magnetic field, lagging slightly behind it.

Two Hall-effect devices are an integral part of the motor. These give sinusoidal output voltages as the rotor turns, and are phased such that their waveforms are 90 degrees apart. Referring to Fig. 1, the scanner drive servo block diagram, the analog-to-TTL converters give logical one outputs, +5V, whenever the output of their corresponding Hall generators are in the positive half cycle. Therefore, a positive zero crossing results in a positive TTL edge, and a negative zero crossing results in a negative TTL edge. Under slowly rotating conditions, when one coil at a time is energized, a negative edge on Hall generator 1 (HG1) occurs when phase 1 is energized, a negative edge on HG2 for phase 2, a positive edge on HG1 for phase 3, and a positive edge on HG2 for phase 4. These edge definitions assume counterclockwise rotation. Fig. 2 shows these time relationships. The zero phase lag waveform for the Hall generators is the slowly rotating condition described above, and the waveforms below those show more typical running conditions, with the rotor lagging somewhat behind the stator field.

Notice that the current waveforms through the windings labeled phase 1 through phase 4 are always in the same place in relation to the counter values listed at the top of Fig. 2. This is because the counter, located in the middle of Fig. 1, is the device that defines where the current waveforms are in the cycle. The output of the

counter addresses the ROMs, which output digital sine and cosine functions. This digital information is then converted to analog waveforms, which are processed to define currents through the coils of the motor as shown. This is the basic drive system for the motor.

Jitter Compensation

The circuitry already described is enough to drive the scanner motor. A problem that remains is a low-frequency jitter which takes about five minutes to damp out after startup. To damp this out faster, a compensation circuit uses phase information to move the poles of the system away from the imaginary axis of the s-plane. This scheme uses a phase comparator to give a signal inversely proportional to the phase lag of the rotor. This signal is ac-coupled into the compensator and conditioned. It is then added to a dc level which sets the peak values of the scanner drive signals. As the phase lag varies, the compensation signal acts to keep the lag constant.

Speed-Detection Circuitry

Included in the speed-detection section are a counter, a latch, and gates to interrupt the machine control processor once every sixteen revolutions of the scanner motor. With this information the processor can tell if the scanner is up to speed or if there is a failure in the circuitry that drives this motor.

Under normal conditions, the 2.4-kHz clock is the input to the counter's clock input. The counter outputs cycle through the ROM addresses, and the ROM data defines sine and cosine waves which cycle at 75 Hz. This data is converted to analog waveforms which are multiplied by the output of a compensator and centered about zero volts. The splitter/current-driver circuit rectifies the cosine wave and drives phase 1 with current proportional to the resulting waveform. Phase 2 is similarly derived from the sine wave, phase 3 from the inverse of the cosine wave, and phase 4 from the inverse of the sine wave.

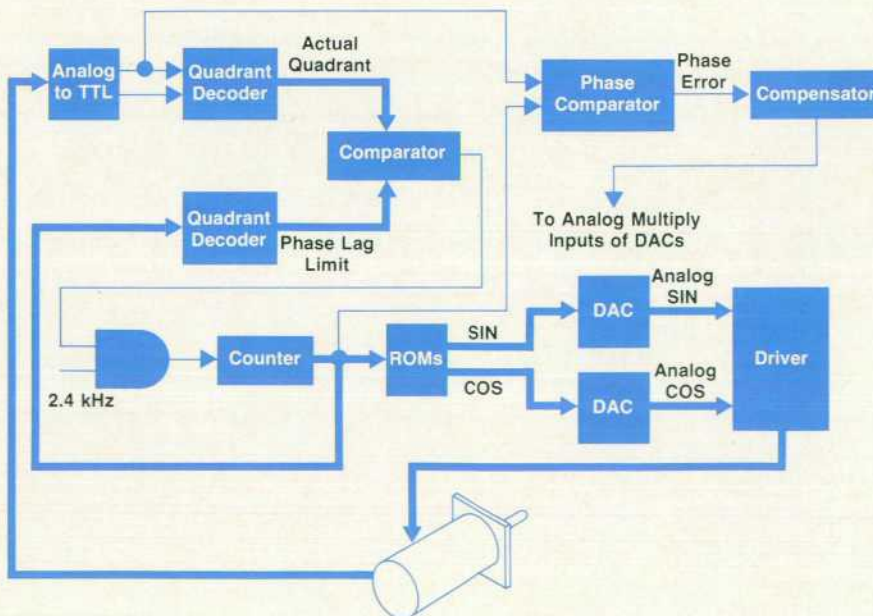


Fig. 1. Scanner drive servo block diagram.

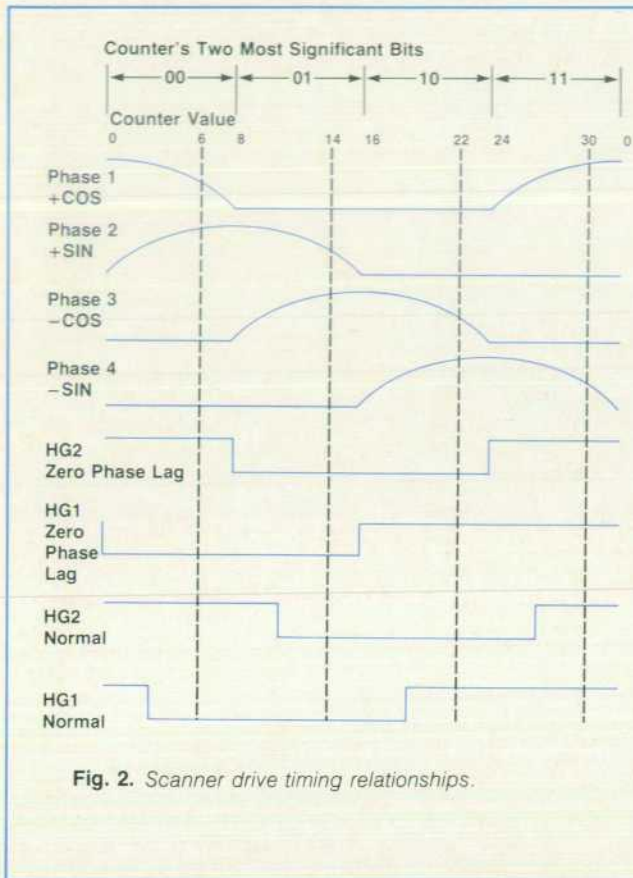


Fig. 2. Scanner drive timing relationships.

Starting the Motor

One cannot simply create a magnetic field rotating at 75 revolutions per second in the stator and have the rotor follow along, because the rotor cannot start to move this fast. Starting is accomplished by beginning to cycle the magnetic field at 75 Hz, but stopping the waveform to allow the rotor to catch up four times per revolution. The four counts on which the waveform may be stopped are 6, 14, 22, and 30. These are indicated in Fig. 2. If the counter is up to six and HG1 is still 1, there is a phase lag of nearly 90 degrees between the stator field and the rotor field. In this case, the clock is disabled until it falls to 0 and is then enabled again. If HG2 is still 1 when count 14 comes along, the clock is disabled until it falls to 0; if HG1 is still 0 when count 22 appears, the wave is stopped until it becomes 1; and if HG2 is still 0 when count 30 is encountered, the clock is disabled until it becomes 1.

Gary L. Holland



Gary Holland was born in Chewelah, Washington and received his BSEE and MSEE degrees from Washington State University in 1976 and 1980. He's been a development engineer and production engineer with HP's Boise Division since 1977. He is listed as inventor or co-inventor on five pending patents related to the 2680A Laser Printer. Gary has taught circuit theory at Boise State University. His interests include amateur radio, woodworking, music, photography, and hiking. He's married, has three children, and lives in Boise.

be referenced to the side surfaces instead of the optical faces.

The last three lenses are held against machined details in the casting as well, but since these lenses are optically thin, they are held by their optical faces. Torsion springs provide pressure in the direction of the optic axis and allow a large tolerance in spring fabrication. A carrier holds the torsion springs for all three lenses, along with screws to cage the lenses. These screws are adjusted during assembly to eliminate clearance but not press on the lenses. The mount slides on a track machined into the casting to simplify assembly (Fig. 8).

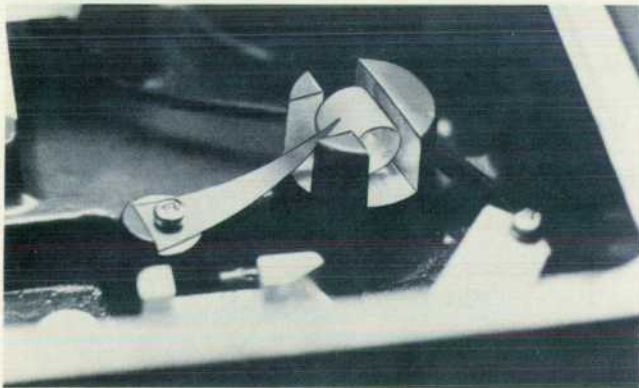


Fig. 7. Leaf springs hold the thicker lenses and the laser in machined slots.

Scanner Drive

In addition to the optical parameters of the scanner, the physical dimensions of the scanning polygon affect the output print quality. The distance from the facet center to the rotational axis must be the same from facet to facet. Any variation in the facet-to-axis dimension shows up as a change in the velocity of the scan and causes printed lines to have a jagged edge on the side away from the synchronization detector.

The polygonal mirror is carefully machined of aluminum so the facet-to-axis distance can be precisely specified, and the mounting detail on the drive motor is ground as the motor is rotating. These methods eliminate a multitude of costly tolerances.

Mirror Mounts

The folding mirrors in the system are adjustable in two axes to allow for some correction of component errors. The first folding mirror aims the input laser beam through the modulator and compensates for errors in the first lens and lens mount. The modulator is adjustable only in the very critical Bragg angle. The adjustments of the second folding mirror further correct the aim and location of the beam through the rest of the system.

An auxiliary mirror is used to send a portion of the beam to a synchronization detector. This mirror is adjustable to allow precise setting of the location of the scan at the drum with respect to the external mounting details of the housing. The exit mirror is supported on one fixed and two adjustable points so that the tilt of the exit beam may be

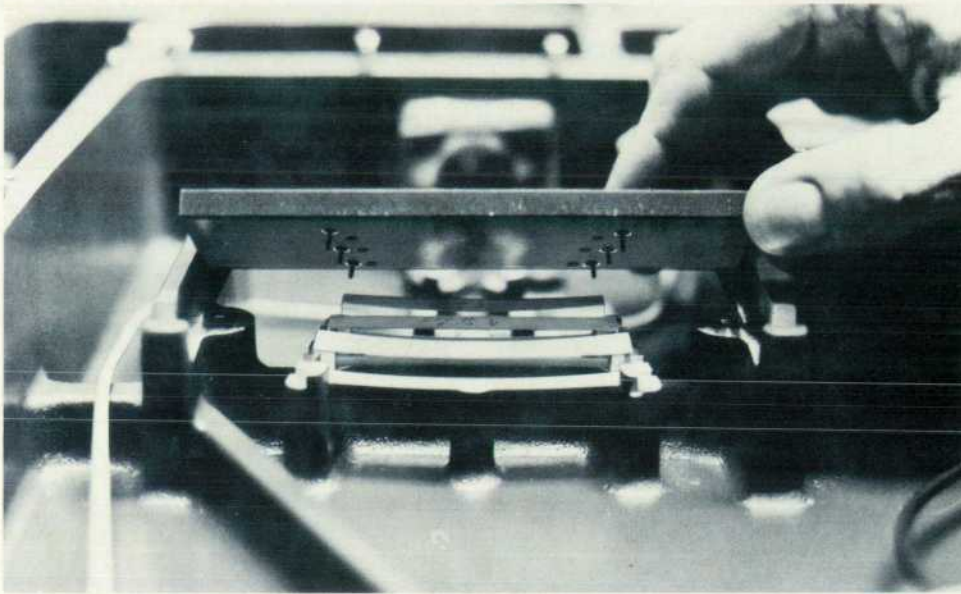


Fig. 8. Torsion springs hold the thinner lenses. The springs are above the plate being held up in this photograph. When the plate is in position, the fingers projecting through the plate press the lenses forward (out of the page) against the posts that can be seen in the picture. The torsion springs can be seen from above in Fig. 6.

adjusted in two directions. Thus the position of the beam at the writing surface is held precisely even in the presence of imperfect optical elements.

Manufacturing and Testing

Since the assembly of the optics module does not allow for adjustment of the lens elements, the mechanical dimensions of the lenses are controlled tightly. This increases the lens costs only slightly and saves a great deal in the cost of mounts and individual element alignment. Each lens is carefully checked for mechanical centering, tilt, and wedge.

A more difficult task is the control of the manufactured dimensions of the housing. This single sand casting is machined with a computer-controlled milling machine so that the large number of tightly controlled dimensions may be reproduced consistently. The number of surfaces and the tolerance levels involved required that even the prototype housings be fabricated on a numerically controlled mill.

The tolerances required to produce the machined hous-

ing are beyond standard manufacturing practice, so a combination of tooling, manufacturing, and inspection improvements were made for this part.

A special operation before the main machining of the part is done to establish a flat, stress-free reference surface. A special setup procedure cuts nonfunctional details on the housing so that the tools may be adjusted according to their actual machining characteristics before cutting important details. This ensures that even the first parts in short manufacturing runs are usable. Each part is monitored after fabrication to return information to the machine operator about how each individual tool is cutting so that cutters may be adjusted or replaced before they produce parts that are out of specification.



Laurence M. Hubby, Jr.

Larry Hubby is a project manager with HP Laboratories. Since 1968, when he joined HP, he has worked on laser interferometers, holography, acoustically tuned optical filters, the 2680A Laser Printer, and optical memories. He's co-author of a paper on optical material properties, an inventor on three optical device patents, and a member of the Optical Society of America. He has taught optics and computer programming. A native of Waco, Texas, he received his BS degree from Stanford University in 1967 and his MS in physics from the University of California at Los

Angeles in 1968. His interests include good food and wine, building and rebuilding "interesting" vehicles, and the visual arts. He's married, has one child, and lives in San Francisco.



John R. Lewis

John Lewis worked on the optics assembly, the frame, the electrophotographic module, and the densitometer of the 2680A Laser Printer. A native of Provo, Utah, he received his BS degree in engineering and applied sciences from California Institute of Technology in 1973 and his MS in mechanical engineering from Stanford University in 1975. With HP since 1974, he worked on solid-state display devices before joining the laser printer project. John is a registered professional engineer in the State of Idaho. He is married, has four children, is active in church activities, and lives in Boise on a one-acre mini-farm where he's restoring an old house and raising animals. He enjoys home computers, classical music, and camping.

CORRECTION

In our June 1982 issue on the 2680 Laser Printing System, Fig. 3 on page 7 shows the laser printer's photoconductive drum rotating the wrong way. The arrow showing drum rotation should point the other way.

Laser Printer Machine Control System

One of two electronic subsystems within the 2680A Laser Page Printer, the MCS monitors and controls the printing process. Its companion subsystem, the data control system or DCS, was described last month.

by James D. Crumly and Von L. Hansen

THE PRINTING MECHANISM of the HP Model 2680 Laser Printing System is monitored and controlled by a microprocessor-based system called the machine control system (MCS). The MCS controls the printing process, paper movement, the operator interface, the electrophotographic process, diagnostics, and most other machine functions. Fig. 1 is a block diagram of the MCS.

The MCS uses an HP-designed 16-bit microprocessor called the MC5.¹ This processor executes a machine control program residing in 32K words of UV-EPROM (ultraviolet-light-erasable programmable read-only memory). There is a 4K-word static RAM (random-access memory) of which 1K is nonvolatile. The nonvolatile RAM contains powerfail information and settable constants for process control. The machine control processor interfaces with over 150 different control devices by means of an I/O bus. Each device resides at a unique I/O address and can be accessed by the microprocessor.

Operating System

The MCS uses a real-time, multitasking operating system to coordinate the control programs. It became apparent at the start of the project that an operating system was neces-

sary because of the complexity of the control required. The control firmware is divided into independent control modules called tasks. The MCS consists of over 100 tasks controlling the operator interface, paper movement, printing, and diagnostics. These independent tasks execute in apparent parallelism, sharing the single MC5 processor. Using a multiplexing scheme, each task executes for a short period of time in a priority queuing structure.

The operating system handles all task-related bookkeeping and coordinates all tasks in the system, determining when a task executes. All tasks exist in one of four states: active, ready, waiting, and dormant. A task currently executing is in the active state. When an active task finishes its work it enters either a dormant state or a wait state. A task entering the waiting state suspends execution temporarily with a request to be awakened after a specified time delay. When the current active task finishes execution the highest-priority ready task becomes the next active task.

Tasks communicate with the operating system by function calls. These calls provided the means for tasks to change from one state to another. The SUSPEND function is used by an active task when it reaches a point where it must wait for an external event. The operating system then puts

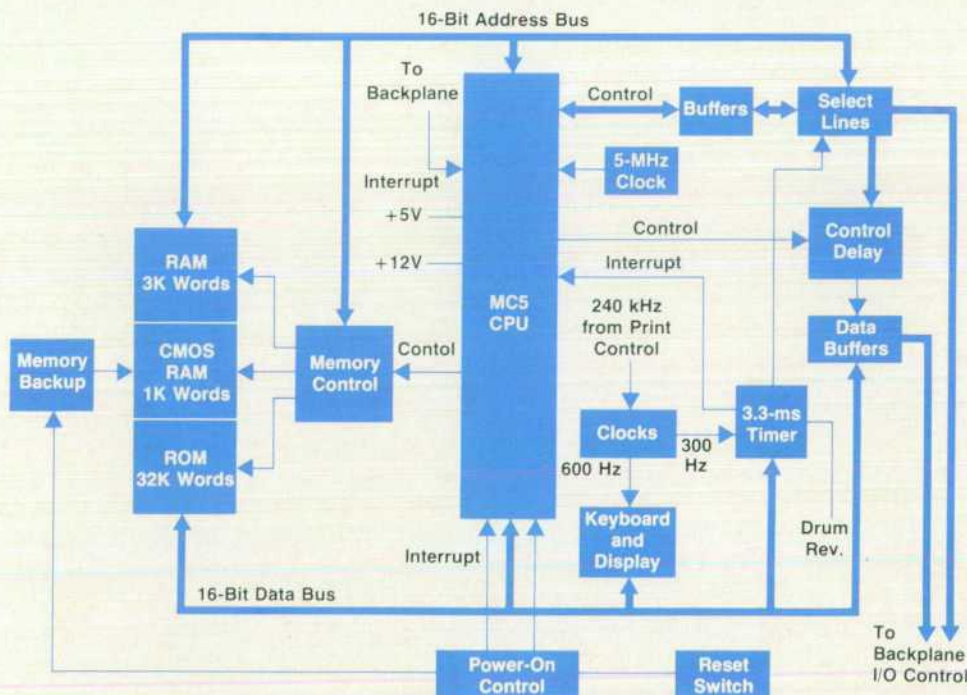


Fig. 1. Machine control system of the 2680A Laser Printer controls drum rotation, paper movement, the operator interface, print density, diagnostics, and other functions.

the active task in a wait state. The suspended task reawakens (enters the ready state) when the suspend time it specified has elapsed. An active task issues a SCHEDULE function when it wishes any other task to enter a wait state with a specified wait time. A DEACTIVATE function call issued by an active task causes a task to enter the dormant state.

The operating system also provides an orderly process for sharing a resource among many tasks. An example of a shared resource is the analog-to-digital converter (ADC) used in the 2680A. An analog multiplexer on the input of the ADC provides input from many sources, and many tasks use the ADC. When a task wants to use a shared resource it issues a SYNCP function call. The calling task is then suspended and its request is queued for the shared resource. The shared resource processes that task's request after processing all the earlier requests in the queue. The requesting task is then reactivated and given the required information from the shared resource.

To minimize operating system bookkeeping overhead, a linked list data structure is used. Tasks are linked with other tasks in the same state. Each task is represented by a block of memory called a task control block (TCB), which contains the information needed to specify a task and its state (Fig. 2). When a task is scheduled its TCB is linked with other TCBs of the same delay time.

There is a circular array of linked list pointers called list heads, with each pointer representing a certain time delay or time slot (Fig. 2). A time pointer points to the list head

representing the current time period. The list head points to the list of tasks ready to execute. At the beginning of each new time period, the operating system advances the time pointer to the next list head. All suspend times are measured relative to the current time pointer. For example, if a task suspends for five time periods, the task's TCB is linked into the list five periods ahead. The maximum suspend time is therefore represented by the size of the circular array of list heads.

Tasks pointed to by the time pointer are in the ready state and are waiting to execute in the current time period. Tasks are positioned in the linked list according to priority information contained in their TCBs. The highest-priority tasks are executed first. If a time period expires before all tasks in the ready state are executed, the remaining tasks are merged into the next list. Low-priority tasks may be pushed back one time slot.

Printing Control

The printing process requires the MCS to perform precise control and timing of a number of machine processes and to synchronize the printing process with the data control system (DCS). See last month's issue for a description of the DCS. A communication protocol is used by the MCS and the DCS to control the flow of pages through the printer. When the DCS has a page ready to print it signals the MCS to start the printing process.

Before the printing process begins the machine must be conditioned for printing. This preconditioning involves such things as warming up the laser, turning on the vacuum system, and starting the laser scanner motor. The preheater is also warmed up and the stacker is positioned to its starting point. The drum is then rotated and its surface potential is adjusted for printing.

Many events during printing require that certain actions be performed at specific drum positions. A drum control task synchronizes events with the rotating drum.

There is 432 mm of usable print area on the 503-mm drum surface. This is enough to print two standard 8½×11-in pages on each drum rotation. The remaining 71 mm is used for electrophotographic process control and the drum seam. During printing, all pages must be within the 432-mm print area. When the DCS has a page to print, a page placement task monitors the drum position and determines when to start the page. When the drum is in the correct position, the MCS signals the DCS to start passing data to the laser.

The page placement task must also furnish information about page placement on the drum so that transfer of the print to the paper can take place at the correct time. The transfer station is approximately one-half drum rotation from the laser position. The transfer control task uses the page placement information to calculate when to start the transfer process.

The transfer control task runs the process of transferring the image from the drum to the paper. This involves the precise control and timing of paper movement, the transfer corona, fusing, and output paper tensions.

After a page is transferred to paper the MCS notifies the DCS that the page was successfully printed on the drum and transferred to paper. The DCS can then release that page from its memory.

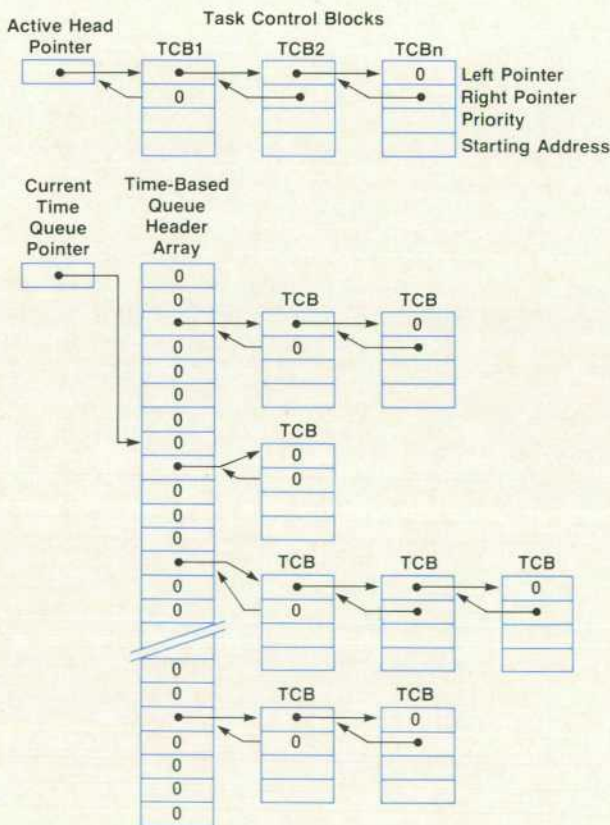


Fig. 2. Machine control system operating system data structures.

Sensing Paper Jams

by Gary L. Holland

The 2680A Laser Printer's paper drive mechanism provides a means for monitoring paper speed and for detecting and terminating abnormal paper motion. The mechanism uses fewer components than methods previously used by high-speed printing devices. Its advantages include higher reliability, lower initial expense, and simpler paper threading.

Fig. 1 is a block diagram of the elements of the paper control and detection system. The speed of the output motor is monitored by a tachometer, which provides a signal proportional to the speed of the motor. This signal is compared with reference voltages in the output motor drive circuit. If the output motor is revolving at an abnormal speed, either a jam-slow detection signal or a jam-fast detection signal is generated. A jam-slow detection signal indicates a paper path obstruction, while a jam-fast detection signal indicates either that the paper has pulled out of the input tractors or the output pinwheels, or that the paper has torn.

The machine control processor described in the accompanying article supplies a maximum-current signal to the maximum-current circuit. This signal sets the magnitude of the current through the output drive motor under normal running conditions. The speed-limit circuit reduces this current to maintain the speed of the motor at a predetermined percentage of normal printing speed, typically 110 percent, when paper is ejected from the printer at the end of a box. The outputs of the maximum-current circuit and the speed-limit circuit are applied to an analog OR gate, which sets the motor-current drive signal to the lesser of the maximum-current circuit output or the speed-limit circuit output.

Speed Limit Scheme

When the paper offers no resistance to the output motor, the speed of the motor tends to increase to an unacceptable level. To prevent this, the speed of the motor is monitored by the tachometer, and if it becomes too high, the speed-control circuit decreases the current through the motor until a preset speed is maintained. This preset speed, at which the speed loop takes over, is faster than normal print speed, but not so fast that inadequate fusing results.

In the speed-limit circuit, the output of the tachometer is low-pass filtered to remove ripple and then compared to a preset level. An error voltage is then input to a compensation circuit which makes the speed-control loop stable and gives it adequate response time. The output of this compensator pulls down the input to the final buffer amplifier to whatever level is needed to balance the power to the motor with the power required to keep the paper moving at a constant speed.

Jam Detection

The jam-detection circuitry in the speed-limit circuit might more properly be called speed-indication circuitry, since the machine control processor must have more information than this circuitry gives to detect a paper jam. The circuit simply compares the output of the low-pass-filtered tachometer signal with a low level to see if the output motor is stopped. If it is stopped, the jam-slow signal is asserted. If the machine control processor knows that the paper should be moving and it sees this signal asserted, it knows that there is a jam condition. The other jam signal, jam-fast, is asserted whenever the speed loop is pulling down the input to the final buffer amplifier. This tells the processor that the paper is not exerting the usual force on the output tractors, which usually means that the paper has pulled out of the input or output tractors or that it has torn. In either case, printer operation is immediately stopped.

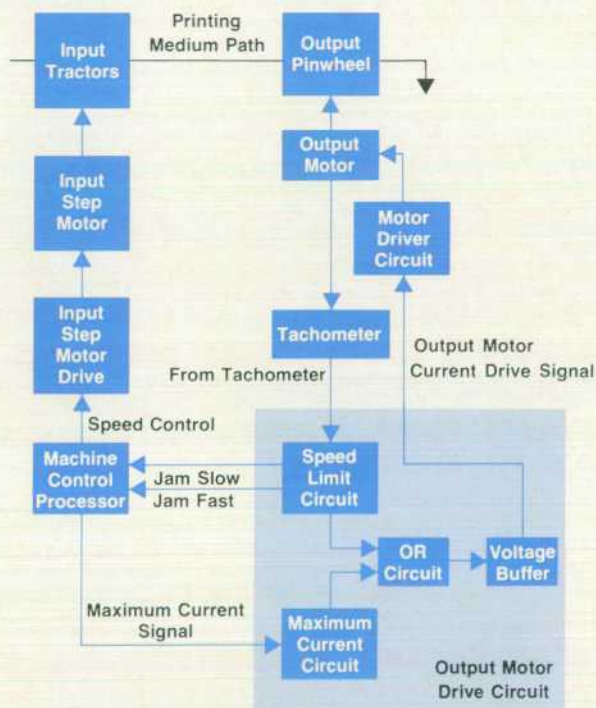


Fig. 1. Paper jam sensing system block diagram.

Keyboard and Display

The operator keyboard, the numeric keyboard, and the 20-character alphanumeric display provide the operator and service engineer with a convenient interface to the printer. The operator keyboard is used to load paper, move the stacker, adjust print registration, eject paper, and print. The alphanumeric display assists the operator by providing information about the state of the machine. The service engineer has access to diagnostic programs and troubleshooting information using the numeric keyboard and the display.

Paper Movement System

The paper movement system controls and monitors the movement of paper in the printer. This system consists of an input step motor, an output tension motor, a position encoder, and a paper jam detection circuit.

The input step motor controls the flow of paper through the machine. A relative-position encoder on the input motor shaft provides feedback to the MCS. This system is designed to keep the paper in registration with respect to print transfer and top of form. During printing the paper position is continually monitored and corrected if neces-

sary so that proper print registration is maintained.

The output paper tension motor applies tension to the paper. The tension value is adjusted according to the needs of various printing conditions. When paper is first started the tension is set to a high value to overcome the static friction of the paper. After the paper is started the tension is dropped to a medium value for printing. When the paper is stopped the tension is reduced to a low standby level.

The output tension motor is also used to detect paper jams (see page 13). The motor contains a tachometer which indicates the tension motor speed. During printing the tachometer is monitored by the MCS to detect jams. If the output tension motor speed is not close to the normal paper movement speed then a possible paper jam condition exists.

Stacker System

The paper stacker system is designed to stack paper automatically during printing and to be used manually by the operator when loading or removing paper. When the machine is not printing the operator can control the stack table using the stack up and down keys. During printing the stacker moves automatically, governed by a special algorithm, to compress the paper stack.

Diagnostics

The first and most important goal of the diagnostics is to minimize the troubleshooting required of the HP customer engineer (CE) when the unit fails, thereby decreasing the mean time to repair (MTTR). It was always foremost in our minds that this product is very complex and uses technologies that are new to HP's service force. Since electrophotography has its historical origins in office products and since the CEs servicing the 2680A are accustomed to dealing with data processing equipment, efforts were made to make the 2680A look as "digital" as possible. Whenever feasible, the diagnostics locate a failed assembly or small set of assemblies and do not require the CE to interpret electrophotographic data.

A second goal of the diagnostics is to reduce the number of special tools and tedious adjustments necessary to service the machine. Sensors included in the system for reliability reasons are used by firmware routines to perform calibrations and adjustments. Procedures that require use of electrostatic potential, development density, and laser beam power measurements are automated by firmware using built-in sensors, eliminating the need for special measurement tools.

A third goal is customer satisfaction. The data processing environment puts some special demands on an electrophotographic device. Typically in the use of a copier, an operator is standing close to the machine when it is printing. If print quality degrades, the problem will be detected almost immediately. The data processing environment, however, is characterized by long periods of unattended operation. Also, the user who is most concerned with the quality of the print may not actually receive the output until long after it is printed. Therefore the printer must be capable of detecting degradations in quality before they become noticeable.

A fourth goal, related to the previous one, is that the

diagnostics should facilitate detection of slowly degrading parts. Since a large part of the cost of servicing a product is in travel to the customer's site, it is helpful if the unit can tell a CE on site what is about to fail so that it can be replaced, saving a separate trip to the site. On the 2680A, data relating to drum potentials and development measurements appears on the diagnostic printout. This data can provide early clues to degradation of the drum or the developer mixture.

Finally, the diagnostics provide tools that were used by the product development team to speed the development of the product. Many of the important operating parameters of the machine were stored in nonvolatile random-access memory and could be changed by entering commands on the numerical keyboard. Thus the operation of the machine could be altered for experiments without having to reprogram the ROM. As the hardware design solidified and the product neared production, many parameters were moved into ROM.

These five goals led to a dual approach to diagnostics on the 2680A: a structured, on-line fault detection system and a set of flexible, off-line, interactive tools.

The on-line fault detection system can detect and report 124 different fault conditions. This system represents the largest portion of the diagnostics in the 2680A machine control system. Most of these diagnostics run continuously as the machine is printing.

Besides adding cost, the addition of sensors and corresponding firmware in the implementation of a fault detection system can potentially decrease the reliability of the overall system by increasing its complexity. To minimize this effect, the 2680A diagnostics take advantage of redundancies in sensing to provide checks on the sensors themselves.

For example, consider a failure of the primary corona power supply. The processor continuously monitors the current to the corona device and the voltage on the primary corona screen. A failure of the power supply first appears to the processor as irregular values for these measurements. The primary corona is used for conditioning the drum, that is, placing a uniform electrostatic potential on it. Therefore the measurement of drum potentials using the electrostatic monitor provides a redundant check on the corona diagnostics. A failure of the primary corona supply causes illegal drum potentials to be measured after some delay caused by the rotation of the drum. The electrostatic closed-loop system attempts to correct the potentials by adjusting the setting on the corona power supply. Since the system is unable to correct the error and the potentials are such that poor print quality would result, the 2680A stops printing with the message, "Hardware Malfunction." A keyboard command can be entered to display the fault message which identifies the primary corona supply as the failed assembly. If a condition had occurred such that the primary corona current and voltage sensors detect a fault but the drum potentials remain in the acceptable range, the 2680A will not stop running and no message will appear. A service representative can enter a command on the numerical keyboard that causes warning messages to appear under these conditions.

Flexible Service Tools

The other approach to diagnostics was to provide a set of flexible tools. By providing a basic set of capabilities that use the numerical keyboard and 20-character LED display, the firmware allows service personnel to deal with failure situations that were not anticipated when the diagnostics were designed. As more is learned about the servicing of the machine from field experience, service procedures can be changed for improved efficiency without altering firmware.

The service keyboard functions are implemented using three-digit keystroke sequences. Access to some of the sequences is controlled by requiring the entry of an access code before certain command sequences will be recognized. The access code is not so much a security feature as a means for protecting the operator from inadvertently altering the operation of the machine or even damaging it.

One class of command sequences allows the display of machine parameters and measurements. Measurements made with the analog-to-digital converter can be viewed, as can running averages of certain measurements. The status of control loops can be displayed to show loop targets and controller settings. Counters that track the age of replaceable parts and the time since the last preventive maintenance can be viewed. Certain parameters stored in non-volatile memory can also be entered as data from the keyboard.

Another type of command sequence can break control loops or disable certain sensors or diagnostics. Analysis of the electrostatic control loop is facilitated by the ability to break the loop and adjust corona settings. A failed sensor can sometimes be circumvented by disabling the diagnostic that uses the sensor, allowing printing to continue until the sensor can be replaced.

Direct control of certain electrical and electromechanical devices in the 2680A can be obtained using the device on/off commands. Solenoids, motors, power supplies, and lamps can be turned on and off individually or in arbitrary combinations by using these commands.

There is also another class of commands that provides miscellaneous tools or automated service procedures. For example, one command displays a log of fault messages that have occurred since the last service call; this can reveal intermittent problems. Another command automates the task of lubricating a newly installed photoconductive drum with toner, prompting the service representative whenever intervention is necessary.

One of the commands that can be entered by the operator is the self-test command. This command causes a printout that can be used for evaluating print quality and that records various measurements and parameters. The self-test diagnostic philosophy on the 2680A is somewhat different from that of other HP printers. The self-test on other printers is a collection of diagnostics which are run only when self-test is invoked. As mentioned above, the fault-detection programs on the 2680A run whenever the machine is printing. Therefore, self-test invokes very few tests that don't run when normal jobs are printing.

Altogether the 2680A provides 190 keyboard commands: 84 display commands, 16 modify commands, 14 disable/enable commands, 48 device on/off commands, and 28 miscellaneous tools.

Reference

1. B.E. Forbes, "Silicon-on-Sapphire Technology Produces High-Speed Single-Chip Processor," *Hewlett-Packard Journal*, April 1977.

Von L. Hansen



Von Hansen was born in Smithfield, Utah and received his BSEE degree from Utah State University in 1976. He joined HP the same year and helped develop the machine control system of the 2680A Laser Printer. Now a project manager with HP's Boise Division, he's a member of the IEEE and is listed as an inventor on two pending patents on 2680A paper control. In 1980 he received his MSEE degree from Stanford University. Von is married, has four children including a set of twins, and lives in Boise, Idaho. He's a member of the Toastmasters speaking club and a small local orchestra, is involved in church work, and enjoys photography, gardening, and woodworking.

James D. Crumly



A graduate of Stanford University, Jim Crumly received his BS and MS degrees in electrical engineering in 1976 and joined HP the same year. He helped design the 2680A corona power supplies and densitometer and worked on the control and diagnostic firmware. He's now a project manager with HP's Boise Division and is a member of the IEEE. Jim is married, has a daughter and lives in Boise. His interests include soccer, skiing, gardening, and Koiné Greek.

Solid-State Microwave Signal Generators for Today's Exacting Requirements

These manually tuned instruments match the extraordinary spectral purity of widely used HP klystron generators and beat them in modulation capability and accuracy.

by Donald R. Chambers and Steven N. Sanders

FOR MORE THAN TWO DECADES the familiar HP microwave klystron signal generators (618A/B/C, 620A/B, 626A, 628A) have been *de facto* industry standards for critical microwave testing. Because their performance was consistent, users considered them standards even though some characteristics essential to the tests at hand were incompletely specified. Now HP has introduced four new solid-state cavity-tuned signal generators that have increased capability and the performance required by today's systems while retaining the characteristics of the klystron signal generators so highly valued by customers. Model 8683A/B (Fig. 1) covers the 2.3-to-6.5-GHz frequency range and Model 8684A/B (Fig. 2) covers 5.4 to 12.5 GHz. The A models are tailored for the communications industry while the B models have high-performance pulse modulation for radar and other applications.

Objectives

The major goal of the generator development program was to match the extraordinary spectral purity of the old klystron generators. It was also desired to incorporate high-quality pulse performance to meet modern radar test requirements, along with AM and wideband FM capability for today's communications industry. It was considered mandatory to achieve better than the current performance in settability and accuracy of output power level and frequency, and it was desired to cover broader bandwidths than older instruments by covering 2.3 GHz to 12.5 GHz with two instruments instead of three to provide a cost advantage to the customer. Self-test was to be included in the instrument to allow efficient use by less skilled operators. Portability and improved drift characteristics were other desired attributes.

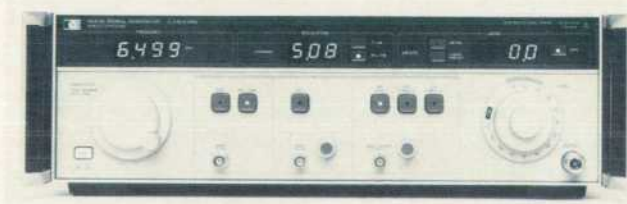


Fig. 1. Model 8683A Signal Generator is a manually tuned microwave signal generator for the 2.3-to-6.5-GHz frequency range. It features excellent spectral purity, settability, and accuracy, and has AM and FM capabilities. Model 8683B offers all these capabilities plus pulse modulation.

The requirement for a CW source free of nonharmonic spurious or subharmonic content and with low sideband noise and drift calls for a fundamental oscillator. At microwave frequencies, best performance is obtained from cavities operating in the quarter-wave tuning mode. However, with the desired bandwidths greater than an octave, it is necessary to ensure that three-quarter-wavelength modes are not excited. To obtain the desired bandwidths, the 8683A/B and 8684A/B oscillator assemblies each consist of two oscillators operating in the same cavity, one for the high-frequency portion of the band and one for the low-frequency portion. The details of these novel designs are given in the article on page 20.

For enhanced level accuracy, some method is needed for compensating for errors that occur outside of the level control loop. By making a microprocessor part of the ALC (automatic level control) system and storing a calibration unique to each instrument, the desired accuracies are obtained.

System Organization

The major features of the instrument configuration are shown in the simplified block diagram of Fig. 3. A straight-through microwave chain is augmented by control and modulation systems.

The microwave chain consists of the cavity oscillator, the amplifiers, the ALC modulator, the output step attenuator, and for the B models, the pulse modulators. While the oscillators deliver significant amounts of power—on the order of +5 to +15 dBm—other parts of the microwave chain have significant losses at microwave frequencies which must be offset by amplification. To ensure that the noise performance is not degraded, the necessary amplification is distributed so there is always a net forward gain in



Fig. 2. Model 8684B Signal Generator covers the 5.4-to-12.5-GHz range. Model 8684A is the same generator without pulse modulation.

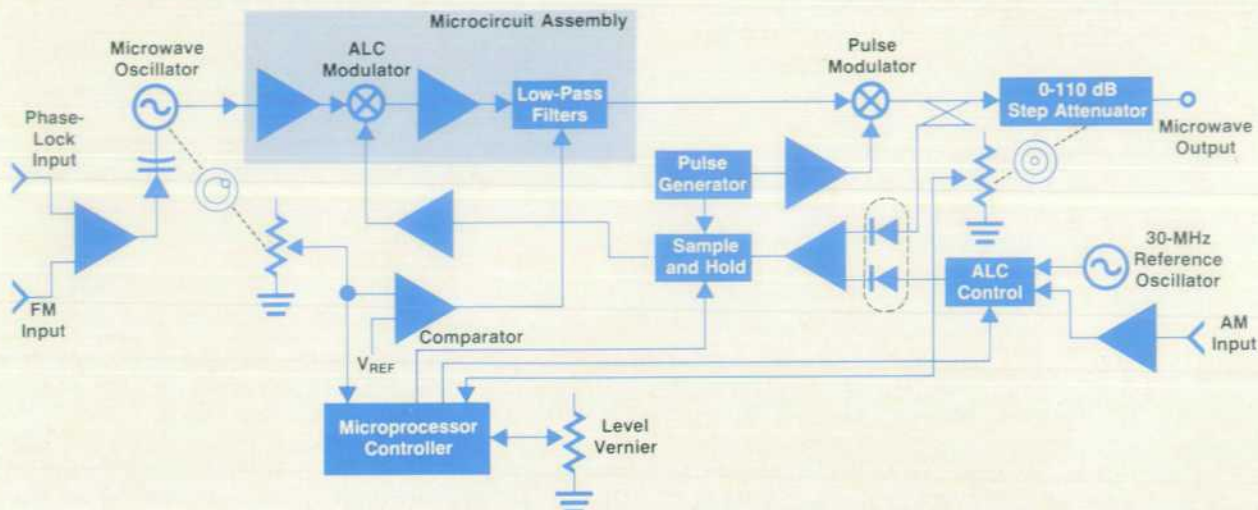


Fig. 3. Block diagram of the 8683B and 8684B Microwave Signal Generators.

the microwave signal path. A proprietary HP FET and thin-film technology allow the two amplifiers and the ALC modulator shown in the block diagram to be included in the same package for a substantial economic advantage.

The ALC modulator and associated control circuitry provide the means for controlling the instrument's output level according to the settings of the front-panel 25-dB vernier and the 10-dB/step manual step attenuator. The ALC modulator also serves to impose amplitude modulation on the microwave signal. To cover all operating conditions, the modulator has 70 dB of attenuation range.

A low-pass filter in the same package as the ALC modulator and associated amplifiers attenuates second harmonics. For output frequencies near the lower band edges the cutoff frequency of the filter is near the midband frequency so the filter suppresses the second harmonic. For output frequencies in the upper half of the instrument's range, the cutoff frequency of the filter is switched to a higher out-of-band frequency.

For the best possible pulse performance, the pulse modulator comes after the final amplification to avoid distortions caused by amplifier ringing or saturation. Including the pulse modulator inside the level control loop provides significant benefits to the user. Dynamic leveling on individual pulses is achieved, and the effects of temperature drift are compensated for, allowing calibrated operation over the wide temperature extremes typically experienced by portable instruments. The ALC system operates over a wide range of conditions, as discussed in the article on page 26.

The block diagram also shows the main control channels in the 8683A/B and 8684A/B. A 6802 microprocessor is the interface between the operator input, the display, and the controlled functions. Except for the mechanical couplings to the cavity oscillator and the manual step attenuator, all other control functions act through the microprocessor/controller.

As indicated in the block diagram, the frequency of the oscillator is sensed by the controller through the position of a ten-turn variable resistor connected to the oscillator tuning shaft. The individual voltage-to-frequency characteris-

tic of each oscillator is determined at final test and stored in EPROM so that each instrument's displayed frequency is characterized individually to better than 1% accuracy.

All ALC functions are coordinated by the controller. To maintain a sufficiently high signal-to-noise ratio in the microwave level sensing circuit, it is necessary to monitor the

Automatic Testing of Manually Tuned Signal Generators

Automatic production testing of 8683A/B and 8684A/B Microwave Signal Generators is done by a desktop computer-controlled test system. The front-panel frequency and power range controls of the unit under test are set by step motors. Front-panel buttons, displays, and other front-panel functions are manipulated through a serial interface similar to RS-232-C between the system controller and the internal microprocessor. The test system measures twenty different parameters as functions of frequency. These parameters include level accuracy, phase noise, pulse on-off ratio, frequency display accuracy, residual AM and FM, and several AM and FM characteristics.

-James Thalmann



Fig. 1. Step motors adjust front-panel knobs for production testing.

power before the step attenuator. Thus the attenuator and other microwave components between the coupler/detector and the front panel are outside of the level control loop.

Since the controller knows the frequency and the step attenuator setting, the internal microwave power level is adjusted to obtain a fixed output level as the frequency is changed. Power level variations caused by the microwave coupler, detector, cables, and attenuator are corrected by the firmware controlling the ALC loop approximately six times per second, reducing flatness errors from about ± 2 dB to less than ± 0.4 dB. The vernier level control is superimposed on this control loop by adding in fixed offsets as determined by the position of the vernier control.

Constant-percentage amplitude modulation is obtained by applying the AM to a fixed 30-MHz reference oscillator and using the ALC loop to force the microwave output amplitude to follow linearly.

When pulse mode is initiated (on the B models only) the internal pulse generator output is applied to the pulse modulator, driving it from the full off condition to the full on condition. In the other modes the pulse modulator is held in the minimum-attenuation condition. To provide leveling on a pulse-to-pulse basis, the ALC uses a sample-and-hold circuit with a bandwidth greater than 30 MHz to handle the 100-ns pulse widths and rise times less than 10 ns. Simultaneous amplitude and pulse modulation is possible, and since FM is introduced at the oscillator, any combination of modulations may be selected simultaneously.

Friendly Firmware Diagnoses Problems

Extensive, easy-to-use diagnostics are designed into the 8683A/B and 8684A/B. Approximately half of the firmware is dedicated to diagnostics.

Twenty-nine critical analog voltages are routed in special shielded layers of the instrument's multilayer motherboard. The microprocessor selects these voltages and performs an analog-to-digital conversion for diagnosing and controlling the instrument. Most of these voltages are used only for diagnosis.

When the instrument is first turned on, the following



Fig. 4. The user can select any of 38 diagnostics by means of the front-panel keys. This test displays a summary of 8683A/B or 8684A/B voltages on a 2600-Series CRT Terminal.

tests are performed:

1. RAM is checked.
2. ROM checksums are calculated.
3. Front-panel communication circuits are checked.
4. All necessary tables are checked for existence.
5. A DAC (digital-to-analog converter) self-test is performed.
6. Eight power supply voltages are checked against limits.
7. Four critical ALC loop voltages are checked against limits.
8. Three frequency calibration potentiometer voltages are checked against limits.

All errors found by these tests are displayed on the front panel during power-up. During five of the tests the microprocessor assumes that the front panel is broken and no communication is possible, so it also blinks a front-panel decimal point to indicate these errors (it has direct control of this decimal point).

User convenience was a major guideline during the design. The user can switch the instrument into a diagnostic mode and select any of 38 diagnostics by pressing front-panel keys. Printed on the inside top cover of the instrument is a block diagram of the instrument and a table that tells what each diagnostic does. The results are displayed in the FREQUENCY digits of the display. Through a serial interface, the user may connect an HP 2600-Series terminal, which allows a more friendly, optional mode of diagnosis. For example, a summary test displays on the terminal's screen the results shown in Fig. 4. These voltages are updated in real-time on the terminal.

If test voltages are outside prescribed limits, the user is notified of the error. In Fig. 4, for example, -30V is out of specification and is underlined on the display.

Some of the diagnosis involves more than limit testing. For instance, 44 flip-flops are tested using passive resistor packages. Thirty-two of these flip-flops connect to a common analog voltage node which is measured by the microprocessor as shown in Fig. 5. The microprocessor first sets all the flip-flops to zeros and measures the common-node "ladder" voltage (V_{low}). Q_0 's low-to-high voltage change is measured by setting only its output to one and remeasuring the ladder voltage (V_{high}). The microprocessor calculates Q_0 's voltage change as $32 \times (V_{high} - V_{low})$.

Each TTL flip-flop's voltage change should range between 2.0 and 5.25 volts. This process is continued for each

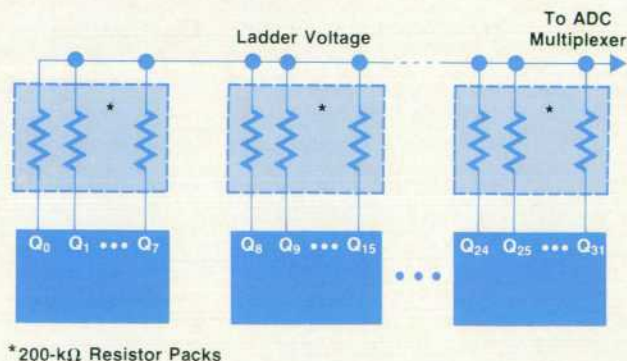


Fig. 5. Method used to diagnose flip-flop packages using passive resistor packs.

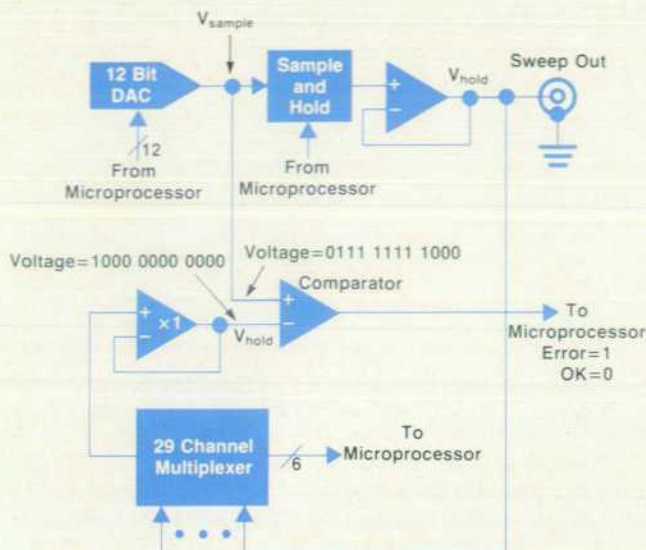


Fig. 6. DAC self-test example. To test bit 11 (MSB): 1) The DAC is set to 1000 0000 0000. 2) The sample-and-hold circuit stores this as V_{hold} . 3) The DAC is set to 0111 1111 1000, or eight bits (40 mV) less. This is V_{sample} . 4) If V_{sample} is less than V_{hold} , bit 11 is all right.

flip-flop, and if an error is found, the board number and IC number are displayed on the front-panel FREQUENCY digits. This method uses small reliable resistor packages that use little power to check complicated flip-flops.

Anything that tests itself might diagnose incorrectly if part of the testing circuitry is faulty. The microprocessor uses the instrument's DAC extensively for diagnosing and controlling the instrument. If the DAC is not working correctly, many false errors may result. Consequently, the DAC is self-tested. The DAC self-test uses a sample-and-hold circuit to store the analog voltage of one DAC setting and then compares that voltage against a different DAC setting, as shown in Fig. 6. Thus the bits check each other. Bits may be connected to ground, to +5 volts, or to each other and the errors will be detected. If all bits are dysfunctional, this will not be detected, but selecting another test, DAC sweep, will show this fault. The three least-significant bits of the 12-bit DAC are not tested because of uncertainties in amplifier voltage offsets.

Operating Firmware

The operating firmware is interpretive and table-driven. It is written in the FORTH language. FORTH's attributes reduced software development time and allowed powerful compiler constructs tailored for this application to be added to the language. The design philosophy dictated that any constant that might change be put into tables that can be changed by production engineers. The following is a list of tables that are individually generated for each instrument.

1. Frequency calibration.
2. ALC level setting.
3. Losses from VSWR and flatness effects of the ALC loop's directional coupler, microwave cables, connectors, the detector diode, and the output step attenuator. This table is a two-dimensional matrix.
4. Frequency flatness for an external RG-214 coaxial cable.

5. FM metering calibration.

6. Limits for diagnostic voltages.

Reliability and economy are enhanced by storing these tables in one factory EPROM on the microprocessor board. There are two empty EPROM sockets to the right of the factory EPROM. The firmware searches for all tables from right to left, and will ultimately find the table in the factory EPROM socket. However, what happens if a calibrated part is replaced, for example an attenuator? In this case, the customer is shipped a new attenuator and a new EPROM with just the attenuator table in it. When this EPROM is installed in one of the empty sockets, the firmware finds the newly installed table first, thereby superseding the old table. All other tables are still found in the factory EPROM. Tables will not have to be consolidated in most cases.

The 8683A/B and 8684A/B Signal Generators use the same firmware, the only exception being their factory EPROM tables.

Donald R. Chambers



Don Chambers received his MSEE degree from Oregon State University in 1960 and spent the next fifteen years as a senior research engineer concerned with microwave theory, components and systems. A member of the IEEE and its predecessors since 1952, he has authored papers on microwave component design and has been with HP for seven years, designing various microwave components and serving as project manager for several instruments including the 8683A/B and 8684A/B Signal Generators. He's a native of Portland, Oregon and a veteran

of two years in the U.S. Air Force. Don has a son, lives in Mountain View, California, races sailboats and works as a volunteer personal counselor.

Steven N. Sanders



Steve Sanders designed the firmware, interfaces, and diagnostics for the 8683A/B and 8684A/B Signal Generators. With HP since 1967, he has contributed to the design of the 8542A and 8580A Automatic Network Analyzers, and he conceived and designed the 84403A Detector for precision network analysis. His work has resulted in one patent. This is his third appearance in the HP Journal. Born in Ogden, Utah, he received his BSEE degree from Utah State University in 1967 and his MSEE from Stanford University in 1970. He's a member of the Sierra Club and the

Hunger Project, enjoys kayaking on the Colorado and other rivers, backpacking (last year it was Nepal), and skiing (both helicopter and the tamer kinds), and is remodeling his fourth house. Professionally, he's interested in the FORTH computer language and automation of the research and design process. Steve is married, has two children, and lives in San Francisco.

Some tables have preambles which define how to use the data in the table. For instance, the attenuator table has in its preamble the starting frequency for the first table entry, the frequency spacing between the data points, a resolution weighting factor, the production date, and other data. Production engineers can modify this table to add more data points across the frequency band, creating a finer correction curve. Thus, they can enhance the flatness as their expertise in building the generators increases. Many more cases exist where production engineers simply modify a table to change a resolution, a range, a gain, an offset, a breakpoint, the effects of pressing front-panel keys, and other functions.

The factory EPROM for the instrument is programmed on a test/calibration system designed especially for the 8683A/B and 8684A/B Signal Generators. The test/calibration system measures the errors of the ALC system mentioned above along with other frequency-dependent errors and programs the EPROM with this unique instru-

ment data. This efficient, automatic process ensures correctness of the data and allows production to specify the control of the table-driven interpretive firmware.

Acknowledgments

The 8683A/B and 8684A/B Microwave Signal Generators are the result of the sustained efforts of many more people than can be listed here. The principal design engineers, other than the authors in this issue, are Calvin Chow and Dieter Scherer (electrical), Chris Rasmussen (mechanical), and Dick Nyquist (industrial design). A special thanks to Callum Logan for the production tooling, to Dave Holmby who made a major effort gathering all the necessary test data during the critical stages of the introduction, and to the production team who made many contributions in the late prototype and early production stages. Special thanks to Harley Halverson, Ron Kmetovicz, and Bill Raukko for guidance and the freedom to do the best job possible.

High-Performance Wideband Cavity-Tuned Solid-State Oscillators

by Edward G. Cristal, Arthur N. Woo, Phillip G. Foster, and Ronald F. Stiglich

AT THE HEART OF THE 8683A/B and 8684A/B Signal Generators are the cavity-tuned microwave oscillators. Why did we choose cavity-tuned oscillators when alternate electronically tunable designs were possible? The answers are spectral purity, frequency stability and economy. Varactor tuning was considered, but microwave varactor Qs are not high enough to meet the strict spectral purity requirements, and varactors have insufficient tuning range. Also, being voltage tunable, varactors are susceptible to noise superimposed on the tuning voltage, which would degrade the signal purity. YIG-tuned resonators were also considered. YIGs have high Q and good selectivity and are capable of multi-octave tuning. Unfortunately, like varactor-tuned circuits, YIG-tuned resonators are very sensitive to electrical noise on the tuning current and are quite temperature sensitive.

The two signal generators must tune over frequency ranges of approximately 2.8:1. Such wide microwave bandwidths eliminated the possibility of using TE or TM waveguide cavities, since these would have had higher-order modes in the bands of interest. Consequently, we decided to use a quarter-wavelength TEM cavity for the 8684A/B oscillator, and a loaded quarter-wavelength TEM cavity for the wide-bandwidth 8683A/B oscillator. The TEM cavity exhibits moderately high Q, hence good selectivity, and spurious-free resonances over a 3:1 bandwidth. The dimensions of the TEM cavities over the 2.3-to-12.5-GHz band

are reasonable from a manufacturing point of view, and can be optimized with respect to cavity Q and higher-order mode suppression.

To achieve the frequency range for the 8684A/B we chose medium-power HP GaAs Schottky-barrier FETs for the active devices. These FETs have $1 \times 500\text{-}\mu\text{m}$ gate geometries, a typical g_m of 45 mS and a minimum f_{max} of 35 GHz. For the 8683A/B it was possible to use bipolar transistors, which have better noise properties than GaAs FETs. The bipolar transistor used in the 8683A/B has $1\text{-}\mu\text{m}$ geometry and is especially developed for low phase noise.

Oscillator Circuit

The oscillator circuit selected for the 8684A/B Signal Generator is the Colpitts configuration shown in Fig. 1. The 8683A/B circuit is the same except that a bipolar transistor is used instead of a GaAs FET and the bias network is different. In Fig. 1, feedback is provided by the capacitive divider made up of the internal gate-source capacitor and the hybrid (internal + external) source-drain capacitor. The cavity resonator, which is used both as a selective circuit and as a matching network, attenuates the harmonic content of the output signal.

All the elements within the shaded area are mounted on a sapphire substrate. The capacitive coupling element is arranged parallel to the tuning rod. The coupling of the microcircuit to the cavity is adjusted by changing the pene-

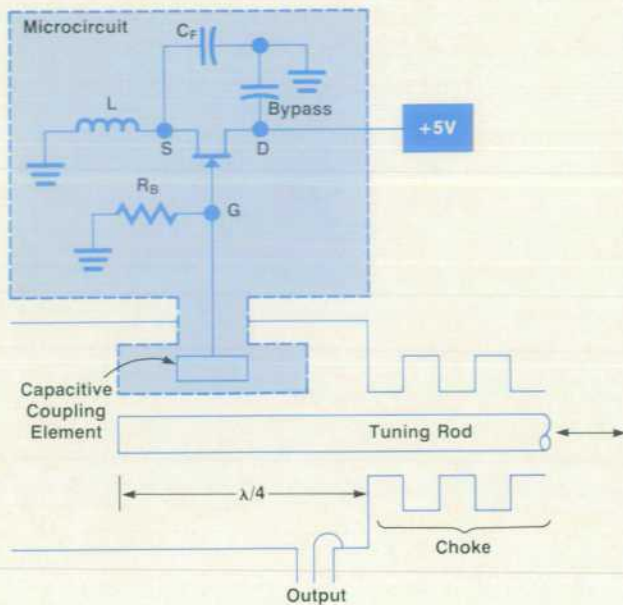


Fig. 1. Schematic diagram of the basic 8684A/B oscillator. The 8683A/B oscillator is similar except that a bipolar transistor is used and the bias network is different. For clarity, only one of the two RF microcircuits is shown and no FM microcircuits are shown (there are two in the 8684A/B and three in the 8683A/B).

tration of the substrate into the cavity. Similarly, the coupling of the load to the cavity is easily changed by adjusting the location of the coupling loop. The inductance L , which is in parallel with the feedback capacitor C_F , imposes a low-frequency limitation on the oscillator. On the other hand, at high frequencies the inductance L could cause additional resonances and spurious oscillations. However, it is possible to build inductors that give broad bandwidth without parasitic resonances in the band of interest.

An innovation in this oscillator design that permitted greater bandwidth than is generally achievable with a quarter-wavelength cavity was to distribute two active circuits along the length of the cavity. Each active circuit is optimized for approximately one-half the total oscillator bandwidth. In this way cavity coupling to one or more active devices is maintained over the entire frequency band. The same concept was applied to the FM microcircuits, thereby yielding broadband FM capability as well. Oscillator power and stability can also be increased by distributing active circuits azimuthally around the cavity. However, this was not necessary in this application. The circuits are mounted on different azimuths, but only to separate them mechanically.

Poor grounding of the sliding center conductor of the coaxial line at the bottom of the cavity can cause erratic tuning. For this reason, we developed a broadband noncontacting choke instead of a simpler but less reliable spring contact system. The choke shown in Fig. 1 consists of low-impedance and high-impedance sections. The choke serves to terminate the cavity with a very low impedance, thereby limiting the cavity resonator length to one-quarter wavelength. The mechanical requirements for the choke are severe, calling for low microphonics, controlled thermal

expansion, and long life.

Frequency Modulation

A typical FM microcircuit is shown schematically in Fig. 2. Two back-to-back varactor diodes mounted on a sapphire substrate are capacitively coupled to the cavity by a coupling element similar to that used for the active circuits. This provides the decreasing capacitance required to obtain flat deviation over the bandwidths of the oscillators. The purpose of the back-to-back series diode configuration is to reduce the generation of harmonics by the varactors. The 8684A/B oscillator uses two FM microcircuits, while the 8683A/B oscillator uses three because of its greater bandwidth. Both of the 8684A/B's microcircuits and two of the 8683A/B's microcircuits are distributed along the length of the cavity. The third FM microcircuit of the 8683A/B is coupled to the center conductor of the cavity resonator at the end of the cavity.

Performance Data

Fig. 3 shows output power as a function of frequency from typical stand-alone oscillators. The minimum power outputs for the 8683A/B and 8684A/B are 2 and 9 dBm, respectively. The entire frequency band can be covered in 20 turns of the front-panel frequency knob in the fast mode, or 200 turns in the fine mode. Frequency settability is typically $<0.005\%$.

The intrinsic FM flatness for both oscillators is about $\pm 10\%$ over most of the bands. However, accuracy of the front-panel FM display is improved to $\pm 5\%$ by using the microprocessor to correct systematic errors. Minimum peak-to-peak FM deviation in both instruments is 10 MHz. The maximum rate is also 10 MHz.

Single-sideband phase noise is one of the most important parameters for a high-performance oscillator. Fig. 4 shows smoothed SSB phase noise data for typical 8683A/B and 8684A/B oscillators in a 1-Hz bandwidth offset 10 kHz from the carrier. SSB phase noise for the 8684A/B is typically less than -80 dBc over most of the band, falling to -75 dBc at the high-frequency end. The SSB phase noise of the 8683A/B is generally much better—less than -87 dBc over the entire band.

Mechanical Design

HP's first microwave signal generator was introduced over twenty years ago and is still going strong. This is a rare

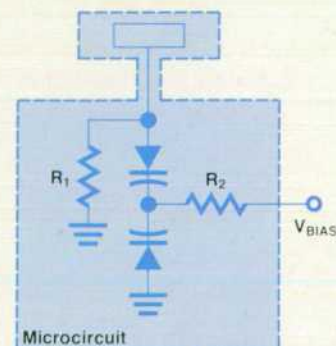
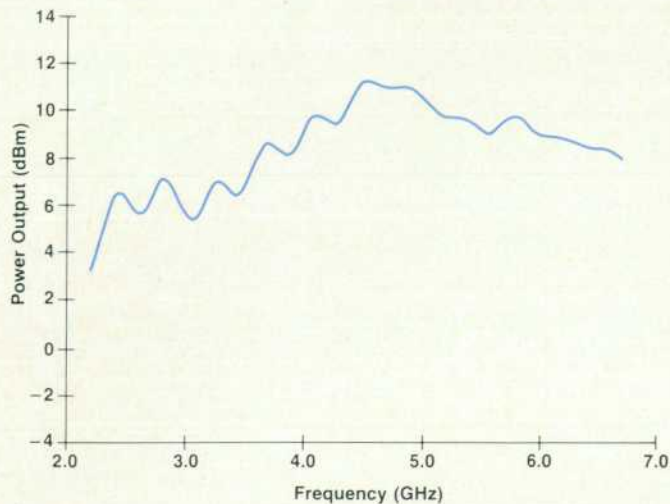
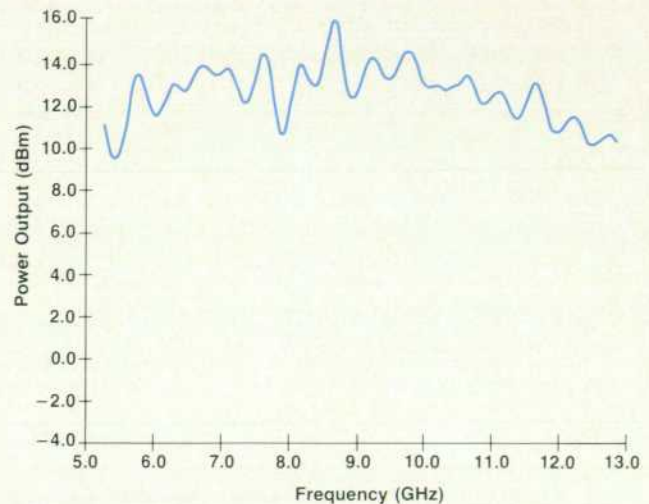


Fig. 2. FM microcircuit.



(a)



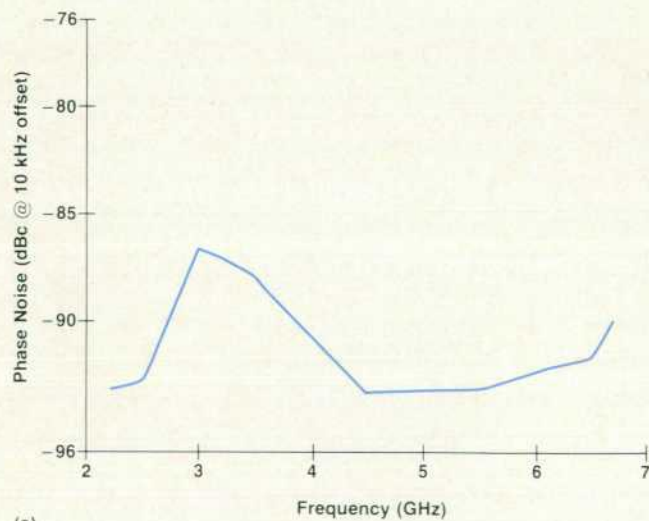
(b)

Fig. 3. Typical power output of (a) 8683A/B and (b) 8684A/B oscillators.

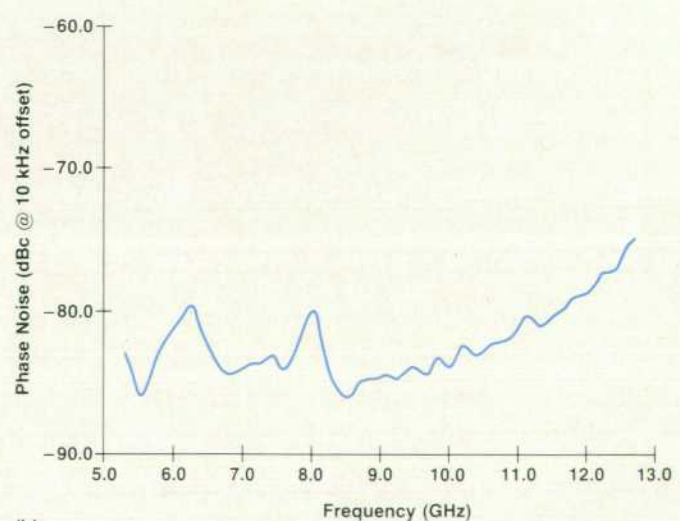
occurrence in the fast-moving electronics industry. A look at the average product lifetime of these generators makes it evident that a proposed replacement must have excellent reliability. Therefore, this was the first requirement for the mechanical tuning mechanism for the cavity-tuned oscillators in the 8683A/B and 8684A/B Signal Generators. We also wanted a cost-effective, durable mechanism that could provide a link between the front panel and the oscillator, giving users the frequency resolution they require. Since there is no scheme for counting the microwave frequency within the instrument, the drive mechanism has to provide the position accuracy needed for an open-loop frequency-determination system. The drive also plays a key role in a thermal compensation design that provides the oscillator with excellent frequency stability over the operating temperature range.

Substrate Mounting

One of the most delicate aspects of the oscillator design was mounting the sapphire substrates. A scheme was developed that allows these substrates to be positioned within the cavity so that assembly is not too time-consuming, but achieves the needed accuracy in positioning these devices relative to the tuning rod. This scheme is shown in Fig. 5. The edge of the substrate is seen in the picture. Attached to the left end is the antenna that couples to the tuning rod. The side containing all the circuitry faces down and rests on two rails. A spring-loaded clip secures the substrate against the rails and another clip compresses the springs to a predetermined height and secures the entire assembly. The left-hand spring applies a greater load to facilitate thermal expansion of the right end in an effort to minimize antenna movement relative to the tuning rod.



(a)



(b)

Fig. 4. Typical single-sideband phase noise in a 1-Hz bandwidth at 10-kHz offset from the carrier. (a) 8683A/B data taken manually at discrete points. (b) 8684A/B smoothed data.

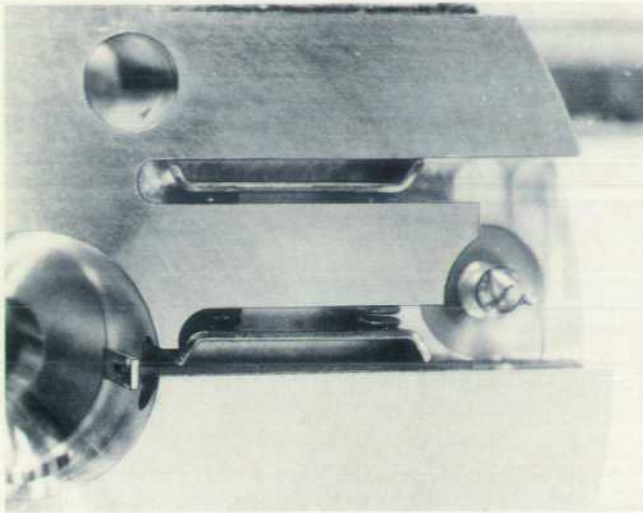


Fig. 5. Spring mounting scheme allows the oscillator substrate to be positioned within the cavity with the required accuracy in a reasonable time.

Precision Frequency Control

Shown in Fig. 6 is a section view of the oscillator and the drive mechanism. The position of the tuning rod determines the microwave frequency of the oscillator. Since the frequency range of the oscillator is measured in GHz and the desired settability is finer than 100 kHz, the incremental accuracy needed in positioning the tuning rod is very, very high. This places a great demand on the bearings supporting the tuning rod. Ideally, one would want to support the tuning rod on both ends and somewhere near the middle. However, the cavity is electrically very sensitive to anything with a dielectric constant greater than that of air, making tuning rod support within the cavity impossible. Behind the cavity is the choke network. The choke is also very sensitive to lossy material. This presented a difficult materials selection problem, that is, to find a bearing mate-

rial that would provide the needed mechanical integrity but not interfere with the low-impedance termination. We chose to use a 20% Teflon™ impregnated acetal resin that exhibits excellent frictional characteristics and has a low microwave-frequency dielectric constant. We found it was still necessary to minimize the amount of material used in each bearing. This resulted in a slotted bearing design that holds the tuning rod over a wide temperature range with imperceptible changes in position. Extensive life cycling has demonstrated that the oscillator will retain its repeatability after long use.

The input shaft of the tuning rod drive extends out to the front-panel tuning knob. The other end is coupled to a two-speed transmission that allows the user to change gearing for either coarse or fine tuning. This is done by simply pushing or pulling on the input shaft, engaging the appropriate gears. The output shaft is connected to a flexible coupling bellows that is secured to the leadscrew. As the user adjusts the oscillator frequency the output shaft turns the coupling bellows, which rotates the leadscrew, which advances or retracts the tuning rod, changing the frequency.

A very linear, accurate potentiometer attached to the other end of the output shaft senses leadscrew position. For any position of the tuning rod within the cavity there is a corresponding potentiometer output voltage. The micro-processor senses this voltage and correlates it with frequency, which is displayed on the front panel. Since frequency is not counted, the potentiometer is responsible for sensing the tuning rod position so that frequency can be inferred. Any sloppiness between the tuning rod and the potentiometer degrades the display accuracy. To minimize these inaccuracies, the flexible coupling bellows is designed with imperceptible windup. The oscillator sealing bellows and internal spring provide loading on the leadscrew to help eliminate backlash, the leadscrew is accurately ground to minimize total composite lead error, and the leadscrew nut is fitted to the screw to eliminate radial

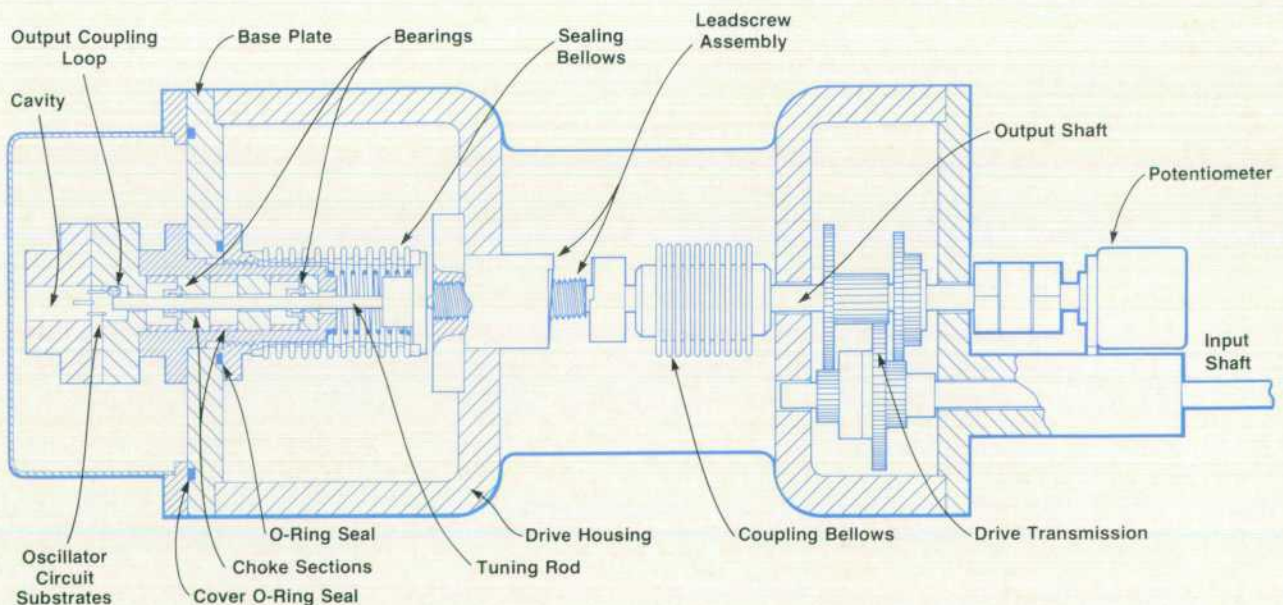


Fig. 6. Section view of the cavity and drive system.

dc-Coupled FM for Microwave Signal Generators

Fig. 1 shows how dc-coupled FM is provided in the 8683A/B and 8684A/B Signal Generators. The front-panel input signal is applied at the input of a resistive network whose gain changes with temperature. The temperature-compensating block then feeds emitter-follower Q1a, which drives the left signal string of shaping diodes. With a low input impedance at Q2a's emitter, the linear FM input voltage is applied across the diodes. Common-base amplifier Q2a diverts the resulting exponential current into load resistor R_L . The voltage across R_L is amplified and passed to the varactors, which couple the FM signal into the tuning cavity of the microwave oscillator (see page 21).

The right string of diodes acts principally as a bias circuit for the left string of signal diodes. V_{CC} draws approximately one milliamper through Q1b, the right string of diodes, diode-connected Q2b, and resistor R_b . Assuming both sides of the circuit are balanced, the resulting voltage at Q2b's base causes one milliamper to flow through the signal string of diodes. As the ambient temperature around the diodes changes, the current in the right string of diodes remains constant. Thus the voltage across the diodes tends to change according to the characteristic diode equation:

$$V = \frac{kT}{q} \ln \left(1 - \frac{I}{I_s} \right)$$

This changing voltage is coupled to the base of Q2a, thereby stabilizing the quiescent current in the signal diodes. On the printed circuit board, the signal and bias diodes alternate, thereby minimizing the effects of temperature gradients on the board. In addition, the temperature-sensitive resistor in the gain block is mounted close to the diodes, allowing it to compensate for the signal diodes' changing incremental resistance with temperature.

The rest of the FM subsystem consists of a video amplifier and metering circuitry. The video amplifier, which is dc-coupled to preserve the dc component of the shaped signal, has two bandwidth-reduction circuits to reduce any phase noise contributions from the FM board when the instrument is not in the FM mode. One circuit reduces the bandwidth of the feedback loop and the other introduces a low-pass circuit on the output of the video amplifier. When FM is selected on the front panel, the amplifier bandwidth extends beyond 35 MHz, thereby allowing for the significant harmonics of the exponentially shaped signal.

The metering scheme features a peak-reading voltmeter that measures the modulation voltage from the FM vernier control on the front panel. Upon command from the microprocessor, the positive and negative peak voltages of the input signal are mea-

sured. The peak voltage is read over a sample time interval determined by the cycle time of the instrument's firmware. Once read, the microprocessor uses an EPROM table of varactor sensitivity versus microwave frequency to compute the FM deviation. The display shows a peak deviation calculated as one-half the peak-to-peak deviation. Since the positive and negative peak detectors are dc-coupled, the true positive and negative peaks are read. Thus the modulation scheme is related to the actual peak voltage and not calibrated to sine waves.

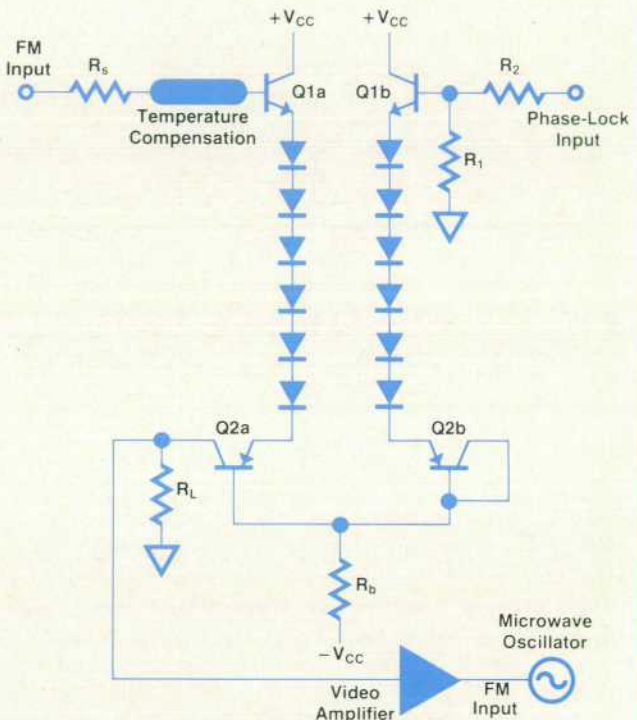


Fig. 1. Frequency modulation input circuit of the 8683A/B and 8684A/B Signal Generators.

A rear-panel phase-lock input is routed through a resistive attenuator into bias transistor Q2b. The resistive divider provides an overall sensitivity of 5 MHz/V and an input impedance over 1 k Ω . Since the FM video amplifier operates at reduced bandwidth when the FM is off, wideband phase locking occurs only when the FM is on.

-James Thalmann

play. This helps to minimize any offset loading of the sealing bellows, eliminating moments that could cause the tuning rod to wander within the cavity.

A cast aluminum housing encloses the transmission and serves as a mount for the oscillator. This housing is secured within the instrument by eight shock mounts that isolate the oscillator from vibrations. This is necessary because the

tuning rod is a resonant, cantilevered beam, so any movement of the rod results in a frequency change. Since mechanical vibrations coupled to the tuning rod result in frequency changes at the rate of the vibration, this would appear as unwanted frequency modulation or residual FM.

Hermetic Environment

The circuits must be protected from moisture and contamination. The cavity side of the base plate is sealed from the environment by an O-ring seal under the cover flange. On the other side of the base plate is a hermetic metal bellows assembly, which provides a flexible seal for transferring the leadscrew motion to the tuning rod. The oscillator is evacuated and then backfilled with dry nitrogen. The final seal is made by tightening the bellows assembly against an O-ring in the base plate.

Temperature Compensation

A desirable feature in most electronic equipment is that performance be flat or constant with temperature. One specification that we actively sought was that the oscillator frequency not vary with temperature. Since the frequency at which the oscillator resonates is a function of how far the tuning rod projects beyond the cavity floor, any change in this distance results in a frequency shift. This distance may be changed by expansion or contraction of the tuning rod and cavity parts as a result of a temperature change.

Referring to Fig. 6, notice that the thermal expansion path of the cavity is quite different from that of the tuning rod. The tuning rod path starts with the leadscrew assembly and includes the bellows, the tuning rod flange, and the tuning rod. The cavity thermal expansion path starts at the leadscrew assembly, continues with the aluminum drive casting and base plate, and ends with the lower cavity pieces. The two paths are designed to minimize the change in apparent length of the tuning rod within the cavity over temperature, thereby maximizing frequency stability with temperature.

The drive housing proved to be an effective variable in the above synthesis. Changes in the length and alloy of the housing helped to minimize frequency drift with temperature. Isolating large expansion contributors and minimizing their lengths and therefore their effects also proved useful.

Precision Machining

Many of the fabricated parts used in the oscillators are critical because they are integral parts of the microwave system. Excellent surface finishes, sharp burr-free corners and edges, and closely controlled fits are required to op-



Ronald F. Stiglich

Ron Stiglich received his BSME degree from Michigan Technological University in 1979 and joined HP's Stanford Park Division as a product design engineer. He was responsible for the mechanical design of the oscillator for the 8683A/B Signal Generator. Ron was born in Plymouth, Michigan and lives in Los Altos, California. He's a avid downhill skier and enjoys backpacking, motorcycles, and golf.



Phillip G. Foster

Phil Foster joined HP in 1957. He has been responsible for the product design of the 140A and 191A Oscilloscopes, the 8601A and 8620A Sweep Oscillators, the 8500A System Console, and the 83001A Microwave Repeater, and for the mechanical design of the 8683A/B and 8684A/B Signal Generators. Before coming to HP he studied mechanical engineering at San Francisco City College and spent four years in the U.S. Air Force maintaining microwave communications equipment. A native of Berkeley, California, he now lives in nearby Los Altos. He enjoys fishing, hunting, and backpacking.



Arthur N. Woo

Arthur Woo received his BSEE degree from San Jose State University in 1972 and his MSEE from Stanford University in 1976. He joined HP in 1979 as an applications engineer with the Microwave Semiconductor Division and from 1976 to 1981 was a design engineer with the Stanford Park Division. He was responsible for the oscillator design for the 8683A/B Signal Generator. A member of the IEEE, he has authored two papers on low-noise amplifiers and transistors and is named inventor on a patent on microwave transistor packaging. Arthur was born in San Francisco and still lives there. He is married, has two children, and enjoys sports, especially baseball and basketball.



Edward G. Cristal

Bud Cristal earned his AB degree in mathematics and BS and MS degrees in electrical engineering from Washington University of St. Louis. He received his PhD degree in electrical engineering from the University of Wisconsin in 1961. After ten years as a senior research engineer and two years as an associate professor at McMaster University, he joined HP Laboratories in 1973. With HP's Stanford Park Division since 1975, he was responsible for the electrical design of the oscillator for the 8684A/B Signal Generator. Bud is a Fellow of the IEEE. He has contributed

more than 40 papers and articles to IEEE journals, has contributed to two books, and is an inventor on two microwave filter patents. He serves as a reviewer for the IEEE Society on Microwave Theory and Techniques and was the recipient of the 1973 IEEE Microwave Applications Award. A native of St. Louis, Bud is married, has two children, and lives in Los Altos, California.

timize their microwave performance. The parts used for positioning the tuning rod and accurately maintaining its concentric location within the choke sections have very tight tolerances. A key factor in the successful production of these parts was the early involvement of manufacturing engineering with the project team. The manufacturing engineers developed precision fabrication processes and determined what new machines would be necessary to produce these parts. Metrology played an important role; initial runs of parts were meticulously measured and the measurements recorded. By reviewing this data we were able to adjust tolerance limits for manufacturing producibility and still maintain interchangeability of these parts. This led to the development of many special gauges needed for production. Materials and alloys were selected to enhance machinability, consistent with microwave performance. Proper heat treating, stress relieving, and handling of these materials is as important as the machining processes in assuring a high yield of precise parts.

Acknowledgments

The authors wish to acknowledge other members of the project team for their contributions to the development of the 8683A/B and 8684A/B oscillators. Robert Joly developed the initial electrical designs and first prototypes. Bill Heinz extended the early prototypes and incorporated the FM circuits into the oscillators. Sandy Smith built the prototype microwave RF and FM microcircuits. Bob Skinner and Klaus Model contributed their skills and ideas to the microcircuit assemblies and fixtures as well as to other areas of the oscillators. Dick Leininger and Callum Logan developed the manufacturing processes for the critical fabricated parts.

A Wide-Dynamic-Range Pulse Leveling Scheme

by James F. Catlin

THE AUTOMATIC LEVEL CONTROL (ALC) system in the 8683A/B and 8684A/B Signal Generators is noteworthy among microwave generators in two principal ways. First, a wide-dynamic-range level vernier provides the convenience of continuous power control over a range an order of magnitude greater than most microwave sources. As a result, the total operating power range of the instrument is broadened without the costly effort of developing a step attenuator with more than the standard 110 dB of control range. Second, by using a sampled feedback technique, pulsed microwave output level is maintained to within 0.5 dB of the CW output under similar operating conditions. Severe duty cycles complicate this task significantly. In human terms, the worst-case specified pulse duty cycle is comparable to waiting a week for a one-minute event to occur. Typical instruments achieve duty cycles comparable to a one-minute event occurring only once every two and one-half months! Under similar duty cycle conditions for pulsed microwave output, it is apparent that synchronization, settling time and hold droop are key concerns in the design of the sampled ALC.

Wide Dynamic Range

A wide-dynamic-range level control is not immediately achievable in conventional ALC systems because of the limitations of the output level peak detector. This component is the most complex in its power level nonlinearities and the most critically affected by ambient temperature variations. Yet signal generators continue to rely on them for output level information because of their simplicity and low cost. It is well known that diode detectors exhibit a square-law response at low power levels and a linear response at high power levels, but there exists no sharp demarcation between the two regions. For this reason, traditional signal generators function at low detector power levels to be assured of consistent square-law operation and are restricted to the smallest dynamic range allowable to prevent detected outputs from vanishing into the system noise. (The output of the detector undergoes twice the dynamic range as the input because of the square law.) In addition, a logarithmic amplifier must follow the detector to provide a linearized correction signal.

The 8683A/B and 8684A/B Signal Generators are not subject to these same limitations, thanks to a novel loop design using two detectors instead of one. Referring to the ALC

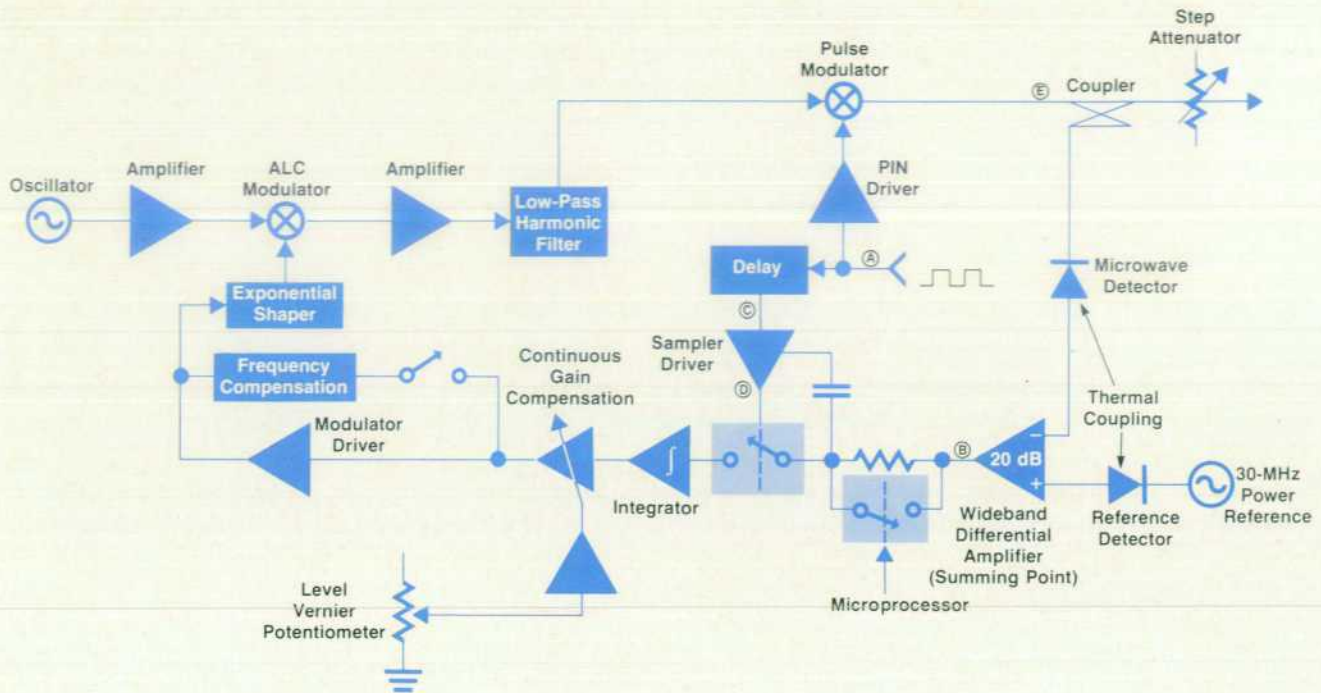


Fig. 1. Simplified diagram of the automatic level control loop of the 8683B and 8684B Signal Generators. The ALC loop in the A models does not contain the pulse modulation components.

loop block diagram, Fig. 1, the summing junction of the feedback system is the 20-dB differential amplifier. This summing point has a reference input and a feedback input like other ALC systems. However, in this configuration, both inputs are derived from detectors. The advantage is simple. If the detectors are similar in sensitivity and the dc loop gain is sufficiently high, then under settled conditions the incident power to the detectors will be equal. This condition exists whether the detector is operating in the square-law region, the linear region, or even the uncharacterized transition region between square and linear. This design allows the addition of an extra 35 dB of level control to the 110-dB step attenuator to cover a total output range of 145 dB, from -130 dBm to $+15$ dBm.

Another advantage of the two-detector system is its inherent temperature compensation. Any temperature fluctuations near the detectors will affect their sensitivity, but thermal coupling between the two detector packages insures that the effect is nearly equally shared. There is no need for elaborate thermistor compensation anywhere in the ALC circuitry. To maintain temperature tracking, the more thermally massive microwave detector contains a hole in its body that completely surrounds the reference detector, which is mounted in a simple TO-18 transistor case. Since neither device generates any heat, there is no significant thermal gradient between devices.

There are, however, two consequences to the double-detector system. Most apparent is the need for an accurate power source to drive the reference detector. The design and function of this power reference oscillator are described on page 28. The other consequence is the characteristic of the control loop to exhibit widely varying open-loop gains as power level is changed, since the detector

diode is in the feedback loop. The ultimate danger here is the possibility of loop instability, but the effect is more commonly perceived as an inconsistency in AM performance, since open-loop gain dictates AM bandwidth.

To address this problem, it is advantageous to identify which system components affect open-loop gain. Normally, any functional block in series in the control loop contributes to open-loop gain in direct proportion to its own small-signal gain. For example, if the microwave amplifier fluctuates in gain by 10 dB across the frequency band of the instrument, so will the open-loop gain of the ALC system. Variations of output power from the microwave oscillator will similarly affect the total loop gain by changing the sensitivity of the modulator inside the ALC loop.

Observing the unlevelled output power, it is not uncommon at these frequencies to see the effects of the microwave components as variations of 15 dB or more over the instrument's operating band. The ALC loop gain can be made insensitive to these variations by incorporating a modulator shaping scheme that produces an exponential control function. As the modulator then regulates power in opposition to these microwave variations to produce a constant output level, it also changes its own small-signal gain proportionally ($d \exp(x)/dx = \exp(x)$), thus maintaining a constant loop gain as well. However, the exponential modulator is not without drawbacks.

Like the ALC detector, the modulator sensitizes the loop gain to output power level in a one-to-one dB correspondence. The customary approach to this compound gain variation is to configure the ALC with a logarithmic amplifier directly following the detector. This was avoided because the log amplifier's rise time depends on signal level, and this would have compromised pulse perfor-

(continued on page 29)

An Accurate RF Power Reference Oscillator

An immediate consequence of the two-detector leveling system described in the accompanying article is the need for an RF power reference. The reference is detected in the same manner as the microwave output signal and the ALC loop forces the signal generator's output level to mimic the power reference. Amplitude modulation of the microwave source can be accomplished simply by modulating this same power reference. Provided that the ALC system has enough bandwidth and dynamic range, the generator will exhibit the same rate and depth of AM as the modulated power reference.

The block diagram of the power reference oscillator is shown in Fig. 1. At its heart is a free-running oscillator that operates at 30 MHz. This frequency is far enough above the highest AM rates (~100 kHz) to be easily filtered out of the carrier after peak detection. However, it is not so high as to preclude the design of simple and accurate RF power generating circuitry. The modulator, peak detector and operational amplifier constitute a local leveling loop that regulates the RF level to hold the RF voltage proportional to the dc input at the inverting input of the operational amplifier. With the peak RF voltage levels after the modulator as high as 10 volts, the operating range of the peak detector can be assumed linear over a wide dynamic range. This signal is stepped down by the transformer to provide proper output levels up to +5 dBm, which can be further attenuated with the -10-dB attenuator. The system microprocessor switches in all but the highest-power range of -10 dBm to +15 dBm. When the user switches from the highest-power range to the next lower range the 10-dB step comes from this attenuator and not the 110-dB output step attenuator. This helps achieve the instrument's 145 dB of

level control using only a 110-dB microwave step attenuator.

Control Signal

The remainder of the circuit provides the control signal used in the local leveling loop as a reference for setting the peak RF voltage. Since it is the RF voltage that is linearly controlled and not the RF power, amplitude modulation is a simple task of summing the external AM signal with the dc reference after proper weighting. The summing amplifier shown near the external AM input combines a stable dc reference with the external AM signal in such a way as to allow a 100%/V influence on the summer's output by the AM signal. Since this voltage is proportional to the RF output voltage, a linear AM capability is achieved with the same external sensitivity of 100%/V.

The output of the summing amplifier is applied to the multiplying digital-to-analog converter (DAC) as a current reference. The DAC output current, scaled linearly to the binary value of the digital ten-bit word from the microprocessor, goes to a current-to-voltage converter which drives a precision voltage divider. One of the four taps chosen by the analog multiplexer from this divider continues on to become the RF voltage reference. With twelve bits to control power level, ten at the DAC and two at the multiplexer, the microprocessor computes the proper digital words to ensure that the output power levels are consistent with the displayed levels. The taps of the voltage divider provide 12-dB steps, while the DAC fills in the fine steps between taps. The fine resolution varies from 0.03 dB/bit to 0.008 dB/bit and appears continuous to the user. Since direct control of the output level is exercised by the microprocessor, corrections for variations in microwave compo-

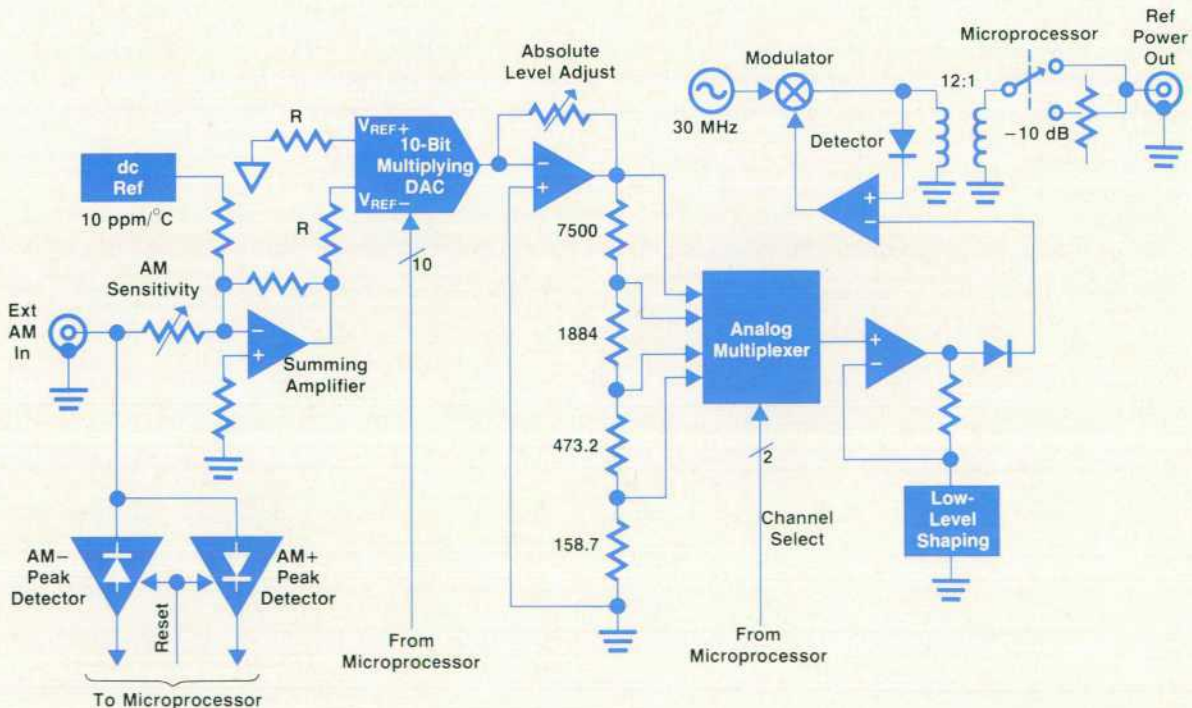


Fig. 1. Simplified diagram of the RF power reference circuit used in the 8683A/B and 8684A/B Signal Generators.

nents such as the attenuator, coupler, and detector are easily implemented by storing them in ROM for the microprocessor to use in its computations.

The operational amplifier following the analog multiplexer buffers the multiplexer channel to avoid voltage-drop errors and shapes the voltage to compensate for detector nonlinearities at low power levels. An offset adjustment here compensates for accumulated dc errors at the local leveling loop.

To display the AM depth percentage for the user the microprocessor periodically reads the voltages of the two peak detectors shown at the external AM input. By measuring both the positive and the negative peak voltages of the AM signal, the microprocessor can eliminate the effects of any applied dc component. The displayed depth is computed from the two peak voltages using the equation,

$$\%AM = \frac{V_{PEAK+} - V_{PEAK-}}{(V_{PEAK+} + V_{PEAK-}) + 2} \times 100$$

To facilitate a fast-falling display of modulation depth, the microprocessor resets the large-time-constant peak detectors after every reading. Hence, a sudden drop in AM signal level will be properly displayed after only two microprocessor instrument cycles instead of the nearly 30 seconds required for nonreset peak detectors.

-James Catlin

mance. Instead, a simple variable-gain element is incorporated following the integrator. Its linear gain is an inverse exponential function of an applied control voltage. A suitable voltage to drive this gain element was easily found in the wiper voltage of the front-panel level vernier potentiometer, thus resolving the loop-gain variations.

Leveled Pulse Power

An interesting feature of the ALC system is the placement of the pulse modulator inside the control loop. Here variations in the insertion loss of the modulator do not contribute to power level variations, allowing the pulse level to be accurately maintained to within 0.5 dB of the similar CW setting. When the microwave power is turned off by the pulse modulator, the feedback system is broken and a hold mode is enabled which maintains the last correct bias level in the ALC modulator until the next pulse arrives. If this were not done, the ALC would respond incorrectly by increasing the microwave level until the average of the detector output became equal to the reference detector voltage. Instead, the sampling switch ensures that the only portion of the signal processed by the system is the flat portion of the pulse waveform after the rising edge has settled and before the falling edge begins. The relationships between the various pulse signals are shown in Fig. 2. Notice the accurate coincidence of the sampling switch drive pulse and the pulse replica from the 20-dB differential amplifier.

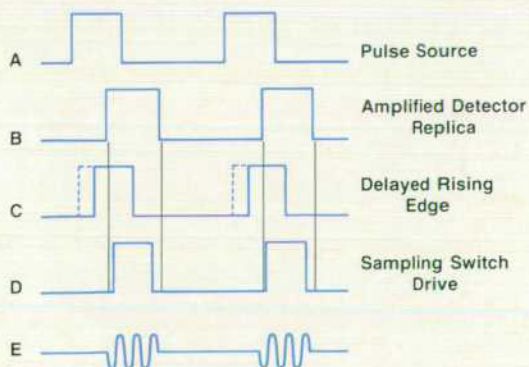


Fig. 2. Timing relationships in pulse mode. Letters correspond to labeled nodes in the circuit of Fig. 1.

In the pulse mode, the system integrator serves as the hold device with a larger-than-normal integrating capacitor switched into effect, while a series FET sampling switch ahead of the integrator breaks the feedback loop when the microwave power is off.

With this sample-and-hold technique, the microwave pulse replica present at the sampling switch must have rise and fall times less than 20 ns to ensure enough sampling window to level a 100-ns-wide pulse accurately. Hence, the detector contains a small (3 pF) storage capacitor and is heavily loaded to provide fast transitions. The 20-dB differential amplifier has a video bandwidth of at least 40 MHz, yielding a rise time less than 10 ns.

Although synchronous operation of the sampling switch and pulse modulator is inherent because of the common pulse signal source, various time delays throughout the system must be equalized to ensure accurate sampling window position. The delay shown before the sampling switch driver is a delay equalizer that predominantly affects only the rising edge of the pulse. While this delay component ensures that the rising edge of the sampling waveform occurs after the replica's rising edge, the microwave path and the 20-dB amplifier provide enough natural system delay to keep the falling edge of the sample pulse well ahead of that of the replica. The result is a sampling pulse that is centered on and narrower than the pulse replica from the detector.

Finally, to keep the offset current of the sampling switch from injecting small packets of charge on every switching transition, an equal and opposite charge injection is accomplished before the sampling switch with the capacitor shown in Fig. 1. To ensure that this capacitor and various parasitic capacitances between the sampling node and the sampler driver are discharged in advance of the pulse level information, a low impedance is connected after the differential amplifier to maintain a low impedance before the sampling switch. This circuit is active only during pulse mode operation.

Acknowledgments

Much of the success of the ALC design is attributable to Bob Batey for his sound foundational work, particularly in the design of the power reference assembly. Thanks go as well to Bud Cristal for theoretical investigations of sampled feedback systems, to Kim Kihlstrom for microwave compo-

(continued on page 32)

Microwave Solid-State Amplifiers and Modulators for Broadband Signal Generators

by Kim Potter Kihlstrom

The amplifier and modulator sections of the 8683A/B and 8684A/B Microwave Signal Generators provide amplitude modulation, pulse modulation, and level correcting capabilities as well as increased power output and isolation of the source from the load. The sections consist of two assemblies. The first assembly contains one stage of amplification followed by a PIN-diode modulator which provides the automatic level control (ALC) and amplitude modulation capabilities. Next in this assembly are three more stages of amplification which increase power output and isolation between the oscillator and the load, and then a low-pass harmonic filter. The second assembly contains another PIN modulator specially designed for pulse modulation (8683B and 8684B only). Each assembly is a separately packaged hybrid integrated microcircuit.

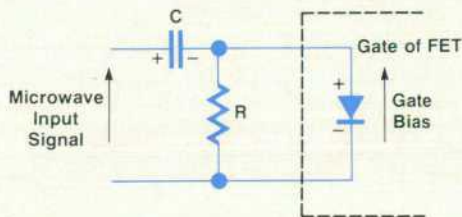


Fig. 1. Gate self-bias scheme.

Circuit elements are typically thin-film (Cr-Au) transmission lines of appropriate impedances and lengths. However, some chip components are used.

One stage of amplification is placed between the ALC modulator and the oscillator to provide about 25 dB of isolation to reduce frequency pulling during normal ALC operation as the modulator impedance changes. The remaining three stages of amplification are placed after the ALC modulator to compensate for its loss and for the loss of the following pulse modulator. The pulse modulator follows all amplification to avoid any amplifier nonlinearities that might be introduced by high-speed switching.

Six different microcircuit assemblies were designed for the four instruments. Different amplifier configurations are required for the

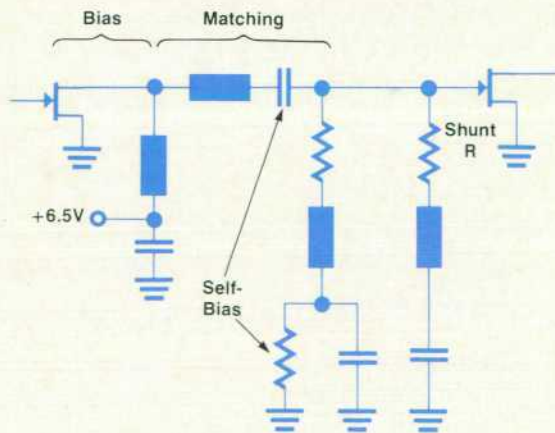


Fig. 2. Interstage coupling network.

8683A and B instruments and for the 8684A and B. Pulse modulators are tailored to the specific requirements of the 8683B and 8684B separately. However, since the amplifiers are functionally similar, as are the pulse modulators, only the details of the 8684B components will be described here.

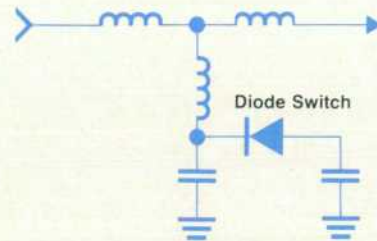


Fig. 3. Harmonic filter equivalent circuit.

Amplifiers

The active devices used in the amplifiers are gallium arsenide Schottky-barrier field-effect transistors (GaAs FETs). The device is an HP proprietary design for medium-power, high-gain applications. It is used in a common-source configuration with 6.5 volts drain bias and a self-biased gate circuit as modeled in Fig. 1. If the RC time constant is much greater than the period of the microwave input signal, the capacitor will charge to the peak value of the input signal and provide the negative gate bias. This arrangement assures that the gate bias is always as small as possible for maximum stage gain.

The FETs are mounted on a gold-plated molybdenum pedestal to obtain good heat sinking and the gate and drain pads are bonded to adjacent substrates (see Fig. 6). The source pads are bonded directly to the pedestal.

Input, interstage, and output matching circuits were synthesized and optimized using computer-aided design techniques. The interstage matching is designed to have a transmission response that increases with frequency to help compensate for the FETs' decreasing gain-versus-frequency characteristic. However, the gain is allowed to retain a somewhat higher value at the low-frequency end of the band to provide a low-pass effect to attenuate the in-band harmonics of low-end signals.

Stability at the low-frequency end of the band is ensured by using a resistive shunt network at the FET gates to reduce the circuit Q. As shown in Fig. 2, the resistor is connected through a transmission line and a blocking capacitor to ground. The trans-

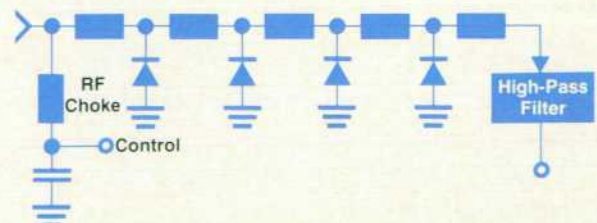


Fig. 4. Basic modulator circuit.

mission line is one-quarter wavelength long at the high-frequency end of the band, effectively removing the effects of the resistor to obtain maximum gain where it is most critical. This improves stability at the low end of the band without a sacrifice in performance at the high end.

To reduce harmonics further, a low-pass filter is included at the amplifier output. To achieve optimum operation over the wide bandwidths of these instruments, the filter cutoff frequency is switched from in-band to out-of-band as the signal frequency is increased. A three-pole Cauer-Chebyshev design is used, as shown in Fig. 3, with the diode to switch the extra capacitance in the leg to ground. The implementation uses transmission lines as lumped-element approximations.

ALC and Pulse Modulators

The basic designs of the ALC and pulse modulators are similar, each having four shunt-connected PIN diodes, as shown in Fig. 4.

The modulators are on when the diodes are reverse-biased. In this condition, the diodes appear as small capacitors and the lengths of the interconnecting transmission lines are picked to match the capacitance for minimum insertion loss. The modulators are off when the diodes are forward-biased and appear as resistors. The dynamic range of the modulators is determined by the minimum forward resistance of the diodes.

The diodes are selected differently for the pulse modulator and the ALC modulator to optimize their respective functions. The pulse modulator diodes are selected for speed of response and low series resistance at forward bias to obtain maximum pulse rise times and on/off ratios. The main characteristic of the ALC modulator diodes is a smooth series resistance as a function of bias current and a dynamic attenuation range of 70 dB.

A curve of typical on/off ratio and a sampling oscilloscope picture of the microwave pulse output for the pulse modulator is shown in Fig. 5.

The output of the pulse modulator is sent through a three-pole high-pass filter to minimize feedthrough of the video control signals used to pulse the diodes.

Fig. 6 shows the microcircuit layout of an amplifier/ALC modulator. The modulator is at the center with the four diodes mounted

on a carrier that functions as the ground plane and the floor of the package. The diodes are shunt-connected between a 50-ohm gold mesh transmission line and the ground plane. A cover over the diodes and the mesh transmission line minimizes signal leakage.

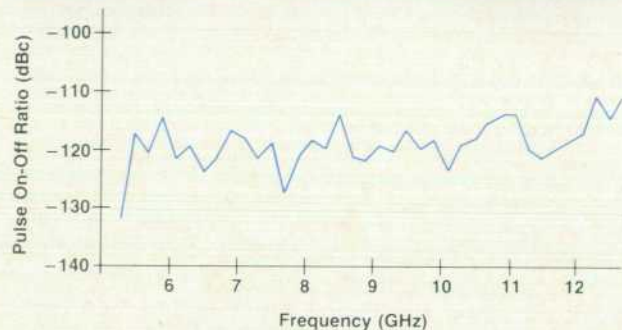
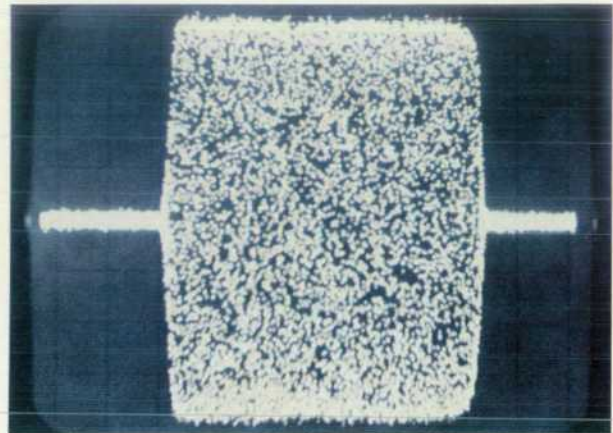


Fig. 5. Pulse modulator performance. Top: A typical 5.4-GHz microwave pulse as seen on a sampling oscilloscope. Peak power = +10 dBm. Horizontal scale: 10 ns/div. Bottom: Pulse on/off ratio for the 8684B.

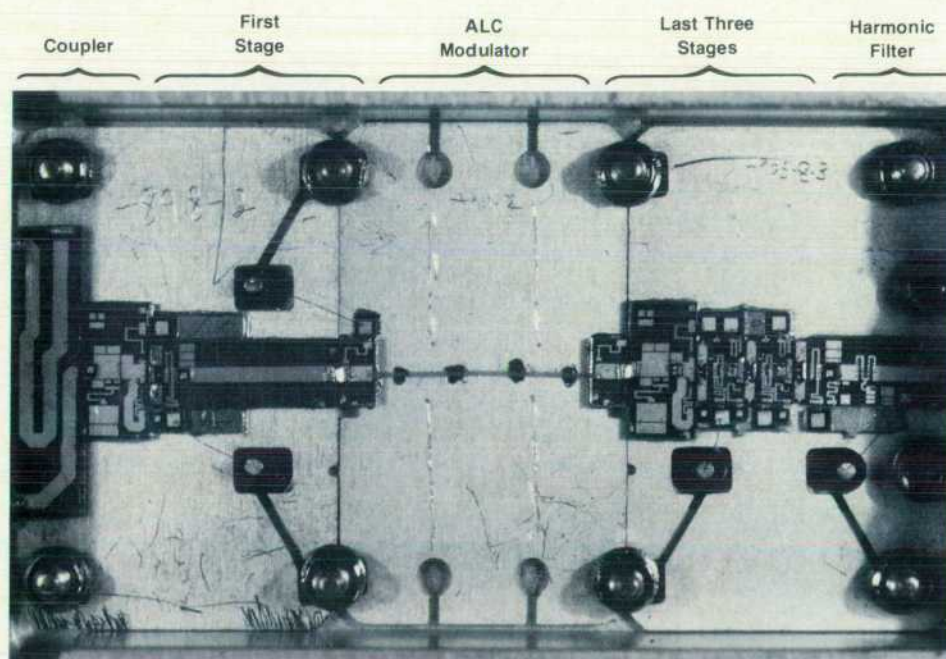


Fig. 6. Amplifier/ALC modulator.

ment characterizations, to Dieter Scherer for technical guidance, to Bob Waldron and Chris Rasmussen for innovative mechanical design of the detector, to Bob Cirner for his expert aid in juggling the over 900 components of the ALC circuitry, and to Phil Hollenhorst for moral support.

Kim Potter Kihlstrom



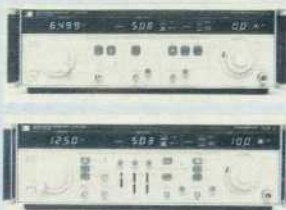
Kim Kihlstrom was responsible for the amplifier and modulator designs for the 8683A/B and 8684A/B Signal Generators. She received her BSEE degree from Stanford University in 1979 and was a development engineer with HP's Stanford Park Division from 1979 to 1981. She's a member of the IEEE. A native of Santa Rosa, California, Kim is married, has a daughter, and lives on campus at Stanford, where her husband is a PhD candidate. She is active in her church and enjoys swimming, tennis, sewing, cooking, and having a daughter.

James F. Catlin



Jim Catlin received his BSEE and MSEE degrees from the University of California at Davis in 1976 and 1978. He joined HP's Stanford Park Division in 1978 and was responsible for the analog design of the ALC system, internal pulse generator, and detector microcircuits for the 8683A/B and 8684A/B Signal Generators. He's now with HP's Spokane, Washington Division. Jim was born in Cheverly, Maryland. He's married, lives in Spokane, and enjoys live theater, kites, and music. Besides being involved in church musical activities, he plays guitar and musical saw. The Catlins are expecting their first child momentarily.

PRODUCT INFORMATION



HP Models 8683A/B and 8684A/B Signal Generators
MANUFACTURING DIVISION:
 Stanford Park Division
 1501 Page Mill Road
 Palo Alto, California 94304 U.S.A.
TECHNICAL DATA: HP Publication No. 5952-8256
PRICE IN U.S.A.: 8683A or 8684A, \$12,000.
 8683B or 8684B, \$15,000.



HP Model 2680 Laser Printing System
MANUFACTURING DIVISION:
 Boise Division
 11311 Chinden Boulevard
 Boise, Idaho 83707 U.S.A.
TECHNICAL DATA: HP Publication 5952-9461
PRICE IN U.S.A.: \$92,000.

Hewlett-Packard Company, 3000 Hanover Street, Palo Alto, California 94304

Bulk Rate
 U.S. Postage
 Paid
 Hewlett-Packard
 Company

HEWLETT-PACKARD JOURNAL

JULY 1982 Volume 33 • Number 7
 Technical Information from the Laboratories of
 Hewlett-Packard Company
 Hewlett-Packard Company, 3000 Hanover Street
 Palo Alto, California 94304 U.S.A.
 Hewlett-Packard Central Mailing Department
 Van Heuven Goedhartlaan 121
 1181 KK Amstelveen, The Netherlands
 Yokogawa-Hewlett-Packard Ltd., Suginami-Ku Tokyo 168 Japan
 Hewlett-Packard (Canada) Ltd.
 6877 Goreway Drive, Mississauga, Ontario L4V 1M8 Canada

020 002 0707 && BLAC & CA00
 MR C A BLACKBURN
 JOHN HOPKINS UNIV
 APPLIED PHYSICS LAB
 JOHNS HOPKINS RD
 LAUREL MD 20707

CHANGE OF ADDRESS: To change your address or delete your name from our mailing list please send us your old address label. Send changes to Hewlett-Packard Journal, 3000 Hanover Street, Palo Alto, California 94304 U.S.A. Allow 60 days.